UPC physics 2023

May 26 – 28, 2023
Asia/Shanghai timezone

Multi-scale Imaging of Nuclear and Proton Geometries

Wenbin Zhao

Wayne State University, Brookhaven National Laboratory

Collaborators: Heikki Mäntysaari, Björn Schenke, and Chun Shen

May. 28, 2023, UPC 2023 workshop, Fudan.

WAYNE STATE UNIVERSITY

JETSCAPE

NSF

Brookhaven National Laboratory

Hydrodynamics response to collision geometry

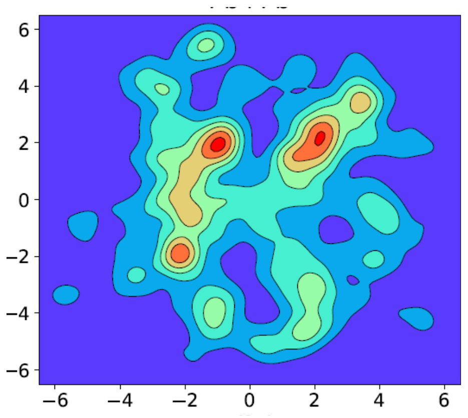

Hydrodynamics

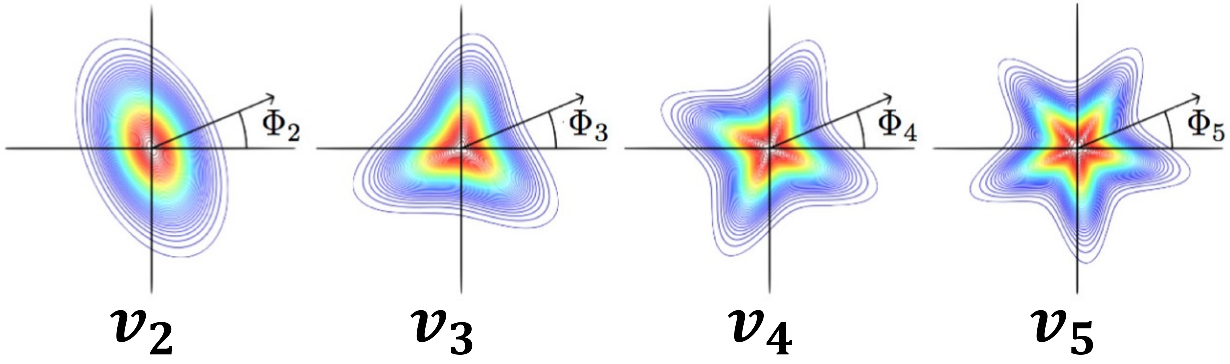

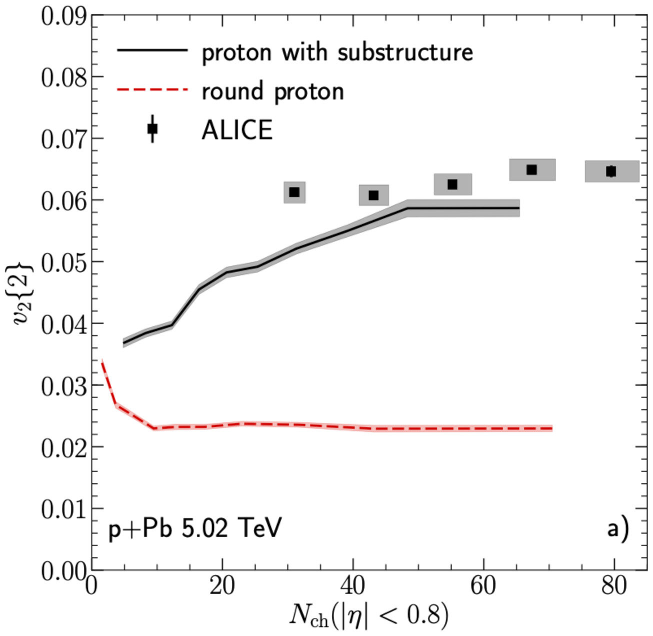

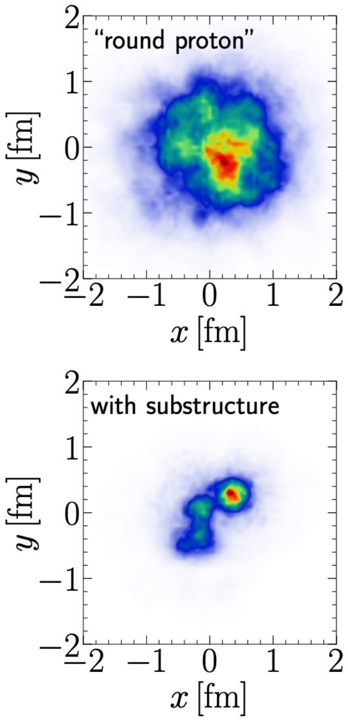

- Heavy-ion Collisions: Initial spatial geometry ⇒ final momentum anisotropy.
- Proton's sub-nucleonic structure is crucial to understand the collectivity in small collision systems

B. Schenke, Rept. Prog. Phys. 84, 082301 (2021).

Diffraction in optics

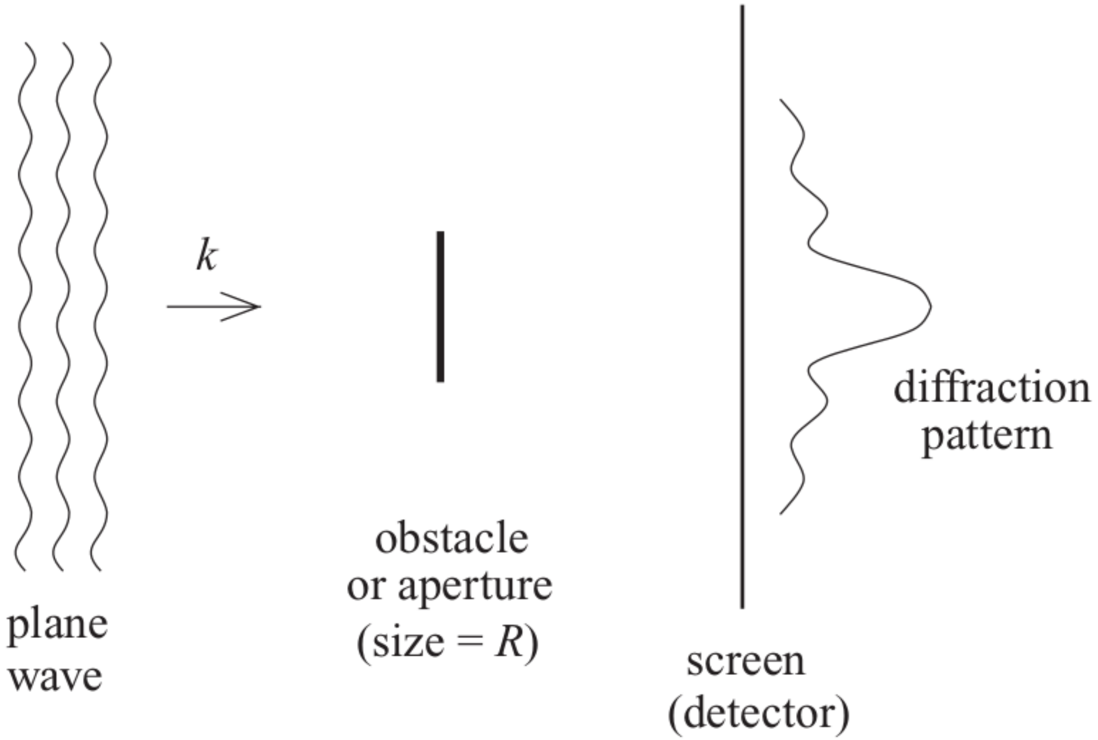

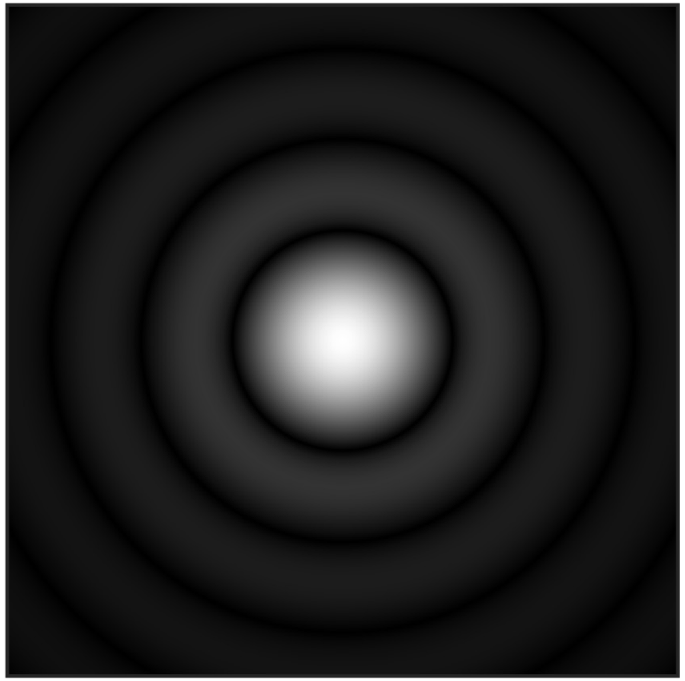

Taken from Wiki

- In momentum-space the positions of the minima and maxima of diffraction pattern are determined solely by the target size R.

Yuri V. Kovchegov, QUANTUM CHROMODYNAMICS A T HIGH ENERGY

Constrain fluctuating proton geometry from DIS

Diffractive vector meson production

High energy factorization:

1. $\gamma^* \to q\bar{q}$ splitting,
   wave function $\Psi^{\gamma}(r, Q^2, z)$
2. $q\bar{q}$ dipole scatters elastically
3. $q\bar{q} \to J/\Psi$, wave function $\Psi^{V}(r, Q^2, z)$

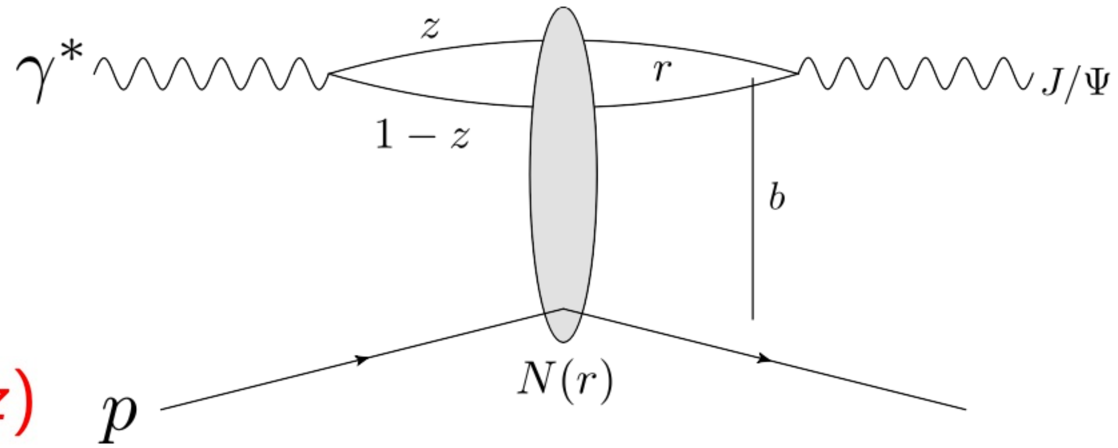

Diffractive scattering amplitude

$$\mathcal{A}^{\gamma^* p \to Vp} \sim \int \mathrm{d}^2 b \mathrm{d}z \mathrm{d}^2 r \Psi^{\gamma *} \Psi^{V}(r, z, Q^2) \mathrm{e}^{-\mathrm{i}\mathbf{b}\cdot\boldsymbol{\Delta}} N(r, x, b)$$

Impact parameter, b, is the Fourier conjugate of the momentum transfer, $\Delta \approx \sqrt{-t}$

N(r, x, b) dipole-target scattering amplitude.

Miettinen, Pumplin, PRD 18, 1978; Caldwell, Kowalski, 0909.1254; Mäntysaari, Schenke, 1603.04349; Mäntysaari, 2001.10705

Dipole-target scattering amplitude (IP-Sat)

$N(\mathbf{r}_T, \mathbf{b}_T, x) = 1 - \exp\left(-\mathbf{r}_T{}^2 F(\mathbf{r}_T, x) T_p(\mathbf{b}_T)\right)$ **accesses to the spatial structure ($\boldsymbol{T_{p/A}}$)**

$F(\mathbf{r}_T, x) = \frac{\pi^2}{2N_c}\alpha_s(\mu^2) x g(x, \mu^2)$. $xg(x, \mu^2)$, gluon density at x and scale μ^2 $(\mu^2 \sim \mu_0^2 + 1/r_T^2)$.

$$\mathcal{A}^{\gamma^* p \to Vp} \sim \int \mathrm{d}^2 b \mathrm{d}z \mathrm{d}^2 r \Psi^{\gamma^*} \Psi^V(r, z, Q^2) \mathbf{e}^{-i\mathbf{b}\cdot\boldsymbol{\Delta}} N(r, x, b)$$

- Diffractive scattering amplitude is roughly proportional to Fourier transform of the spatial structure function of target (Tp/A).

Miettinen, Pumplin, PRD 18, 1978; Caldwell, Kowalski, 0909.1254; Mäntysaari, Schenke, 1603.04349; Mäntysaari, 2001.10705

Coherent and incoherent processes

- **Coherent** $\sigma_{\text{coherent}} \sim |\langle \mathcal{A} \rangle_\Omega|^2$

Target stays intact, (<initial state| = |final state>)
Probes the average shape of the target.

- **Incoherent** $\sigma_{\text{incoherent}} \sim \langle |\mathcal{A}|^2 \rangle_\Omega - |\langle \mathcal{A} \rangle_\Omega|^2$

Target breaks apart, (<initial state| ≠ |final state>)

Probes the variance of event-by-event initial state fluctuations in target structure.

- Experimental signature: rapidity gap.
- Theoretically: no net color transfer.

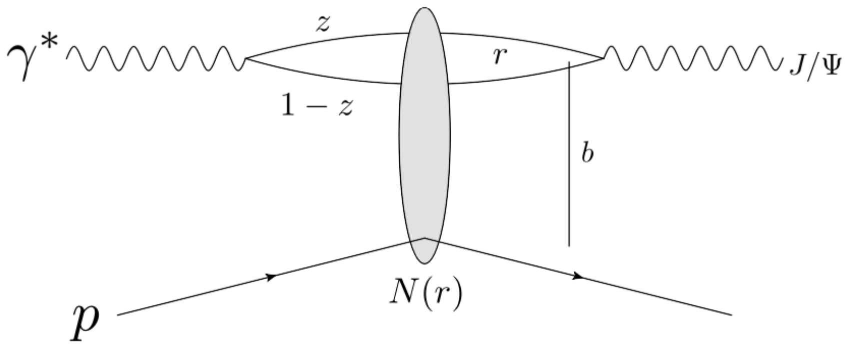

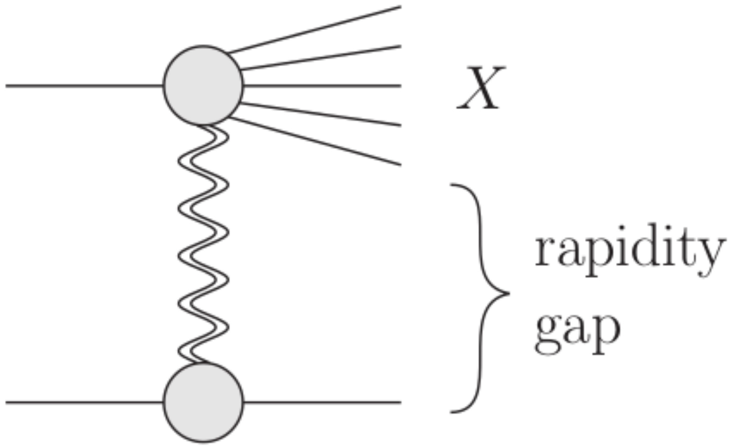

Miettinen, Pumplin, PRD 18, 1978; Caldwell, Kowalski, 0909.1254; Mäntysaari, Schenke, 1603.04349; Mäntysaari, 2001.10705

Proton geometry fluctuations

- Proton's event-by-event fluctuating density profile:

$$T_p(\mathbf{b}_\perp) = \frac{1}{N_q}\sum_{i=1}^{N_q} p_i T_q(\mathbf{b}_\perp - \mathbf{b}_{\perp,i}), \quad P(\ln p_i) = \frac{1}{\sqrt{2\pi\sigma}} \exp\left[-\frac{\ln^2 p_i}{2\sigma^2}\right].$$

- The density profile of each spot is:

$$T_{\mathrm{q}}(\vec{b}) = \frac{1}{2\pi B_{\mathrm{q}}} e^{-b^2/(2B_{\mathrm{q}})}$$

- The spot positions $\overrightarrow{b_i}$ are sampled from:

$$P(b_i) = \frac{1}{2\pi B_{\mathrm{qc}}} e^{-b_i^2/(2B_{\mathrm{qc}})}$$

Schenke , etc.al. PhysRevLett.108.252301 ,
PhysRevC.86.034908, Mäntysaari, Schenke, 1603.04349;

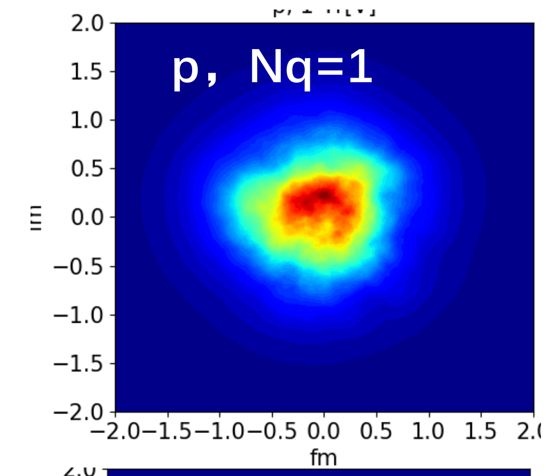

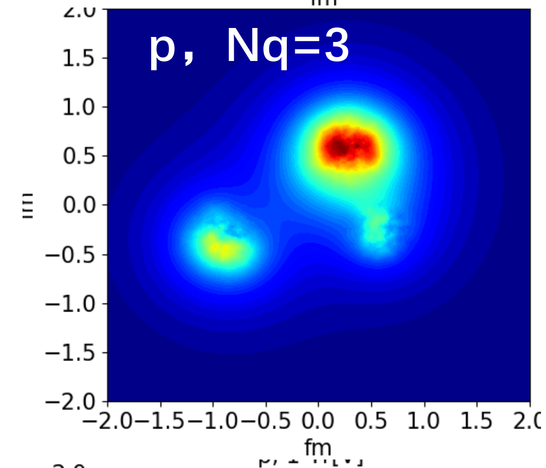

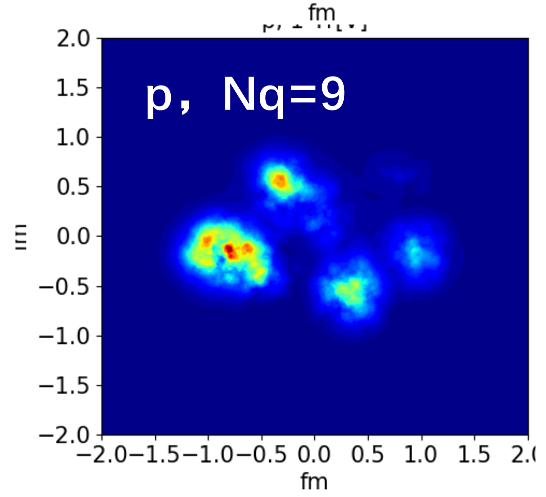

Model parameters and the Exp. Data ($\gamma^* + p \rightarrow J/\psi + p^*$)

Parameterize proton shape (T_p)

- Number of hot spots N_q
- Proton size B_{qc}
- Hot spot size B_q
- Hot spot density fluctuations σ
- Min. distance between hot spots $d_{q,min}$
- Overall color charge density: $Qs(x)/g^2\mu$
- Infrared regulator m

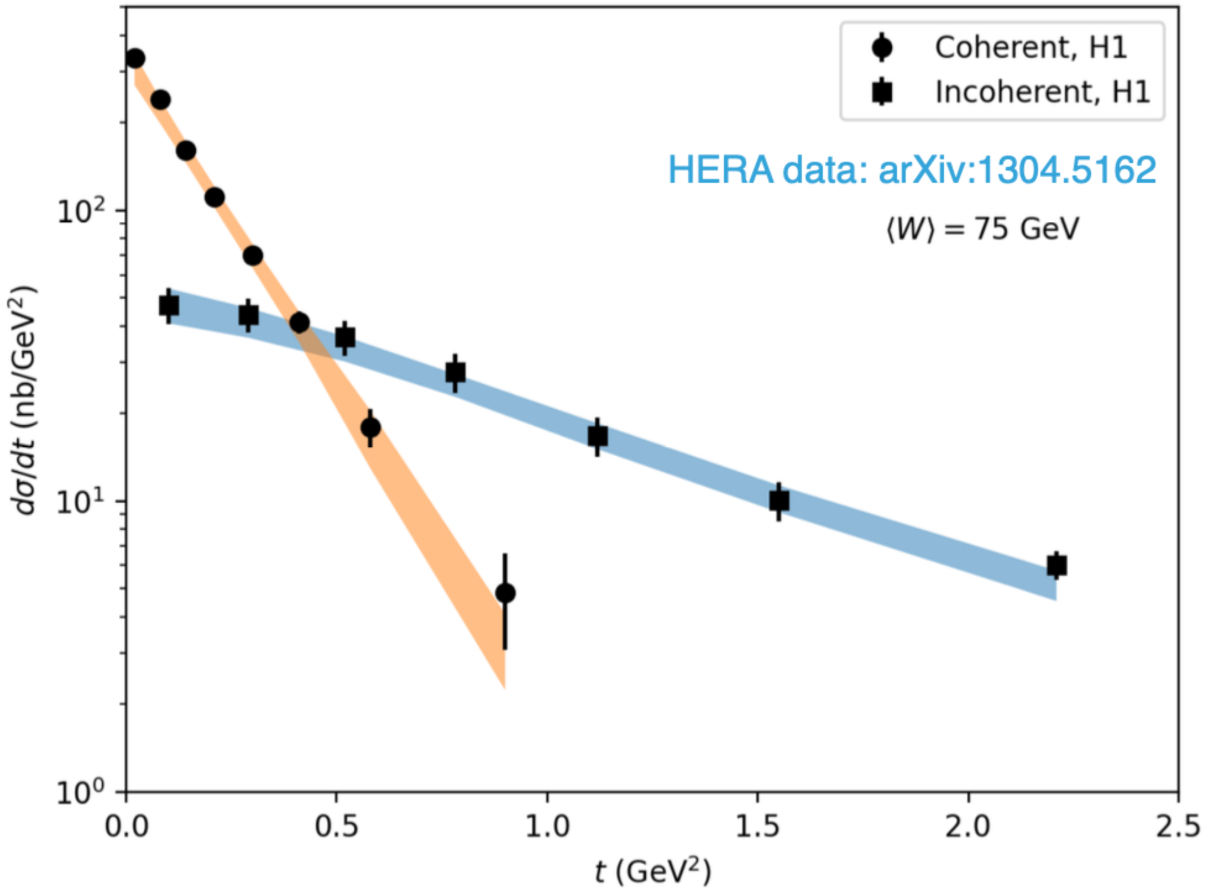

- 7D parameter space; generated 1000 training points for the model emulator

H.Mantysaari, B.Schenke, C. Shen and W. Zhao, Phys. Lett. B 833 (2022), 137348.

Posterior Distribution

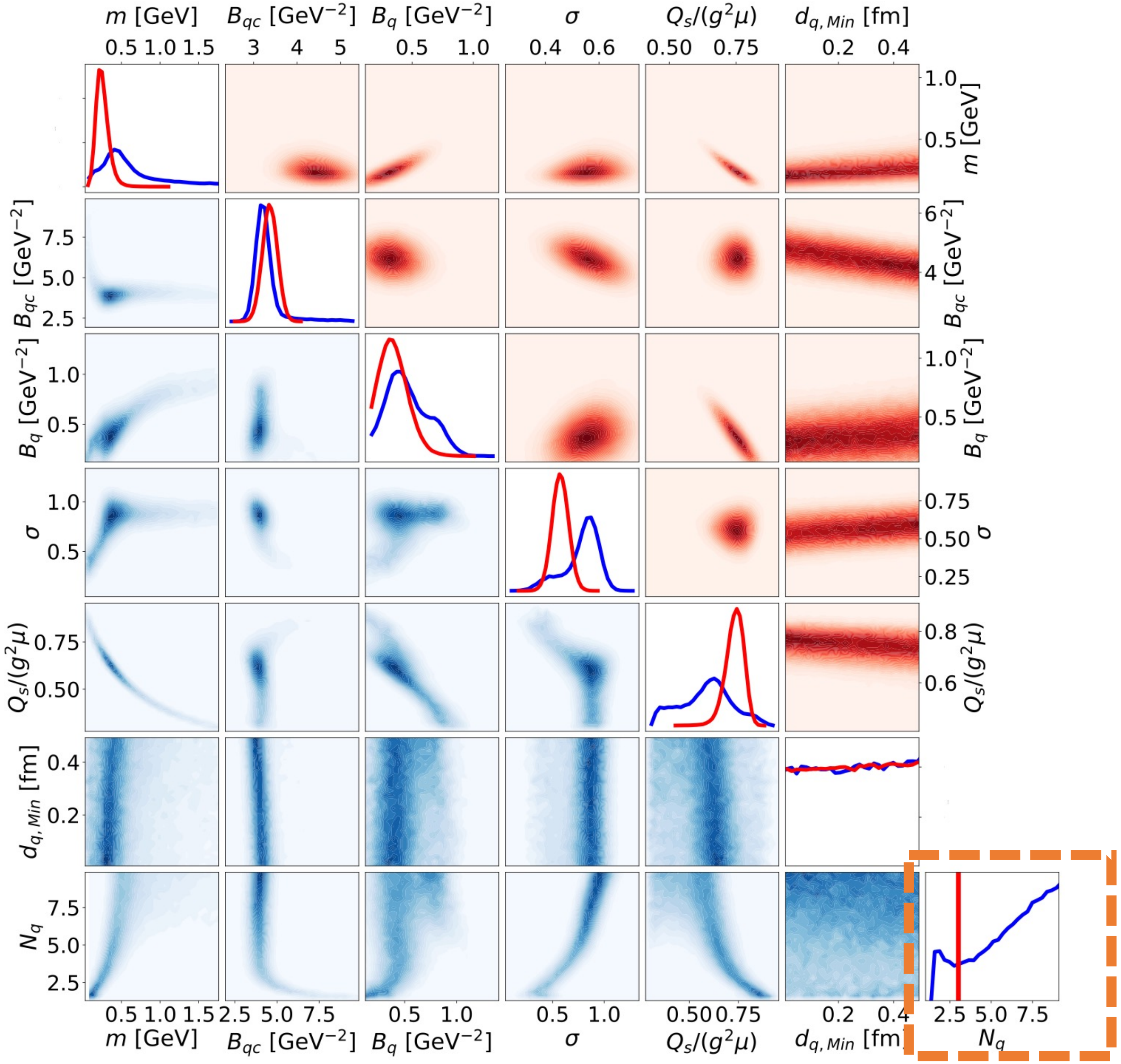

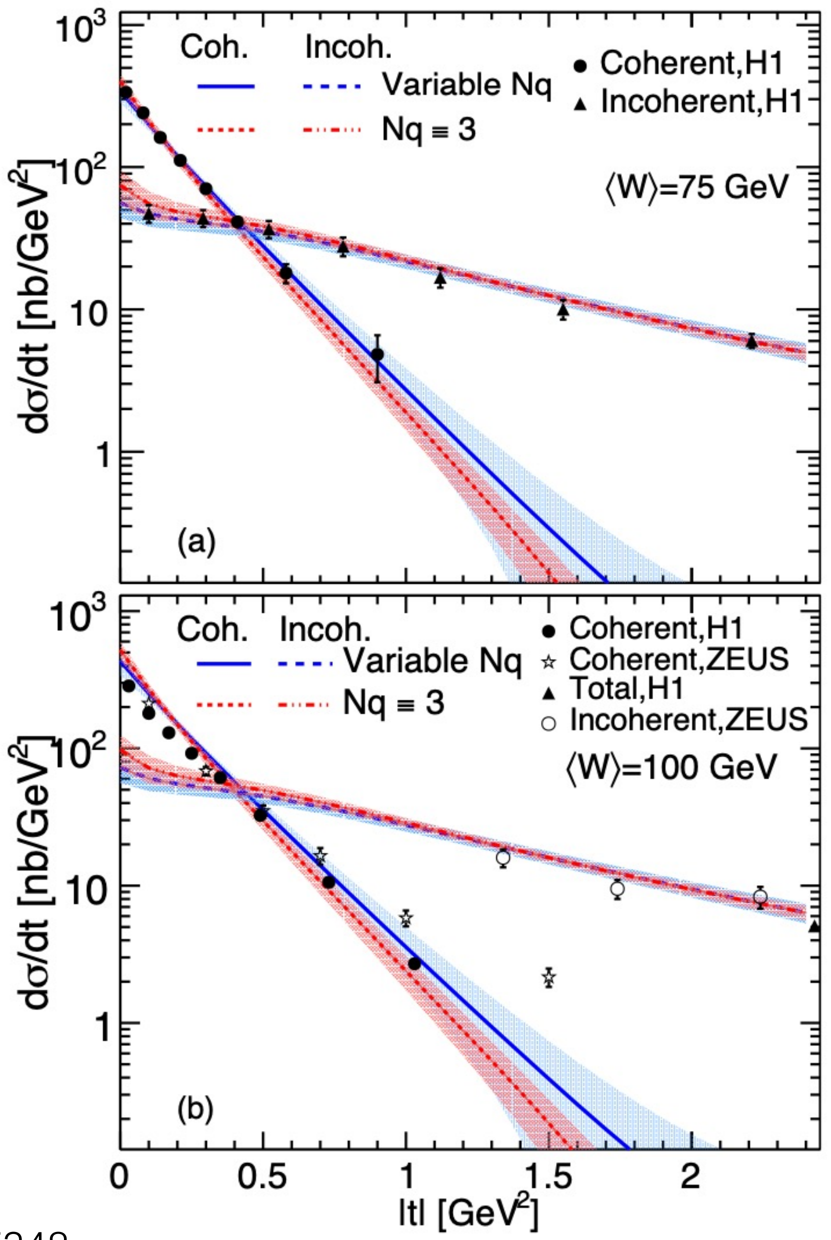

H.Mantysaari, B.Schenke, C. Shen and W. Zhao, Phys. Lett. B 833 (2022), 137348.

Proton & hotspot sizes at high energy

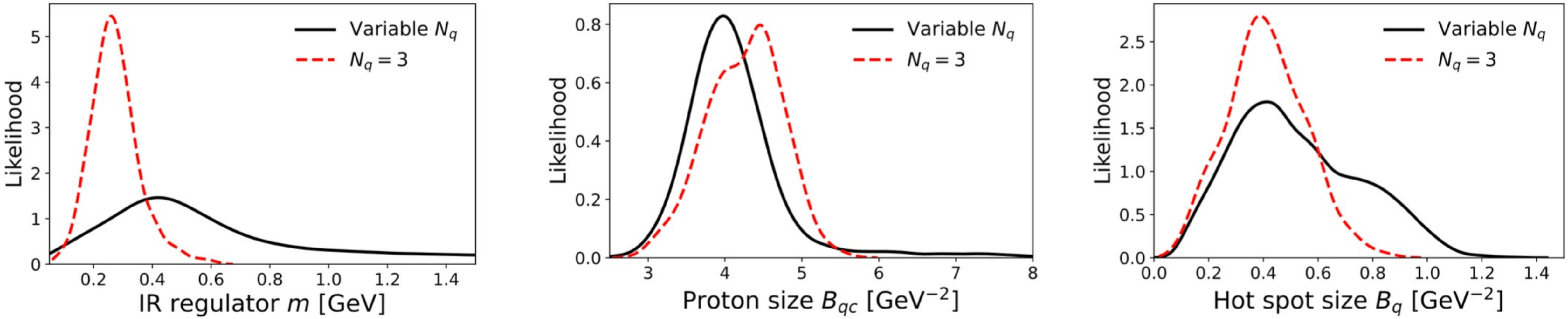

- Some parameters are well constrained .
- The 2D RMS proton radius $R_{rms} = \sqrt{2(B_{qc} + B_q)} \sim 0.6$ fm, which is consistent with the results in heavy-ion collisions.

H.Mantysaari, B.Schenke, C. Shen and W. Zhao, Phys. Lett. B 833 (2022), 137348.
H.Mantysaari, B.Schenke, C. Shen and W. Zhao, [arXiv:2208.00396 [hep-ph]].
G. Giacalone, B. Schenke and C. Shen, Phys. Rev. Lett. 128, 042301 (2022)

Degeneracy in the number of hot spots

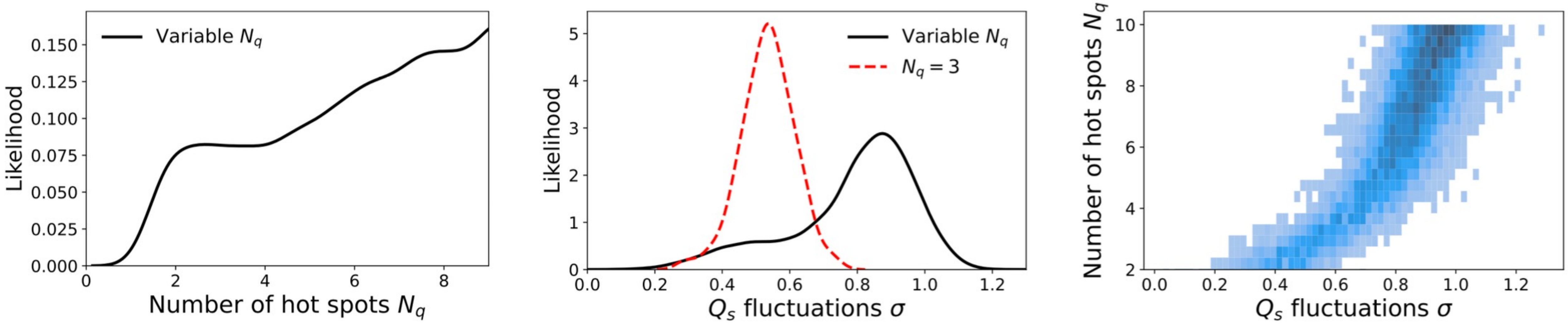

- The likelihood of number of hot spots Nq increases monotonously.
- Large Nq partially compensated by large Qs fluctuations, $\sigma \propto \sqrt{N_q}$, "number of effective hot spots" < Nq
- **Proton's event-by-event fluctuating density profile:**

$$T_p(\mathbf{b}_\perp) = \frac{1}{N_q}\sum_{i=1}^{N_q} p_i T_q(\mathbf{b}_\perp - \mathbf{b}_{\perp,i}), \quad P(\ln p_i) = \frac{1}{\sqrt{2\pi}\sigma}\exp\left[-\frac{\ln^2 p_i}{2\sigma^2}\right].$$

H. Mantysaari, B.Schenke, C. Shen and W. Zhao, Phys. Lett. B 833 (2022), 137348.
H. Mantysaari, B.Schenke, C. Shen and W. Zhao, [arXiv:2208.00396 [hep-ph]].

MAP of fixed Nq=3 and Nq=9

Parameter	Description	$N_q = 9$	$N_q = 3$
m [GeV]	Infrared regulator	0.780	0.246
B_{qc} [GeV^{-2}]	Proton size	3.98	4.45
B_q [GeV^{-2}]	Hot spot size	0.594	0.346
σ	Magnitude of Q_s fluctuations	0.932	0.563
$Q_s/(g^2\mu)$	$Q_s \Rightarrow$ color charge density	0.492	0.747
$d_{q,\mathrm{Min}}$ [fm]	Min hot spot distance	0.265	0.254
N_q	Number of hot spots	3	9
S	Hydro normalization	0.1135	0.235

- The Nq=3 and Nq=9 have the different configurations at large length scales.
- “See” them by the different probes.

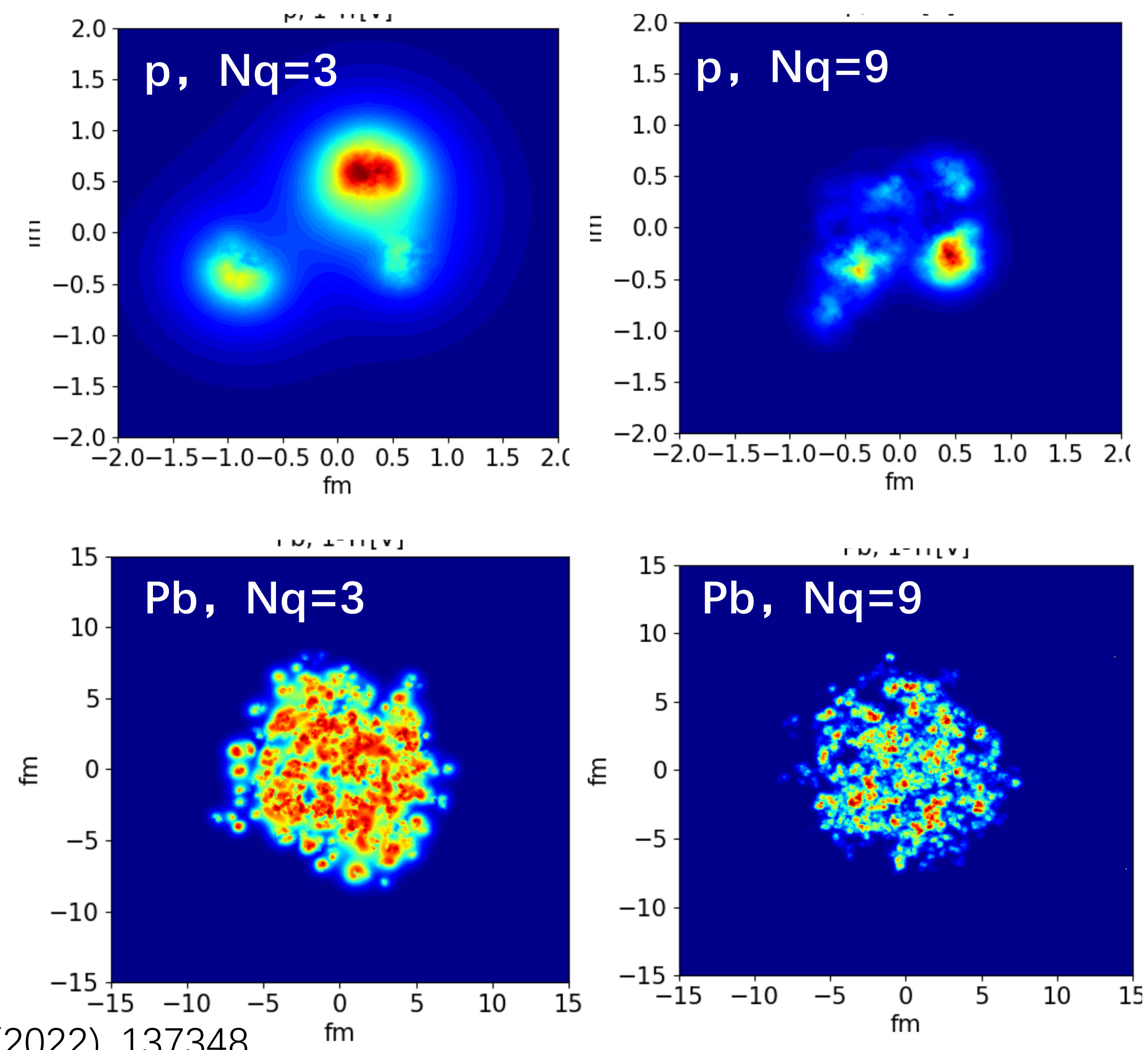

H. Mantysaari, B.Schenke, C. Shen and W. Zhao, Phys. Lett. B 833 (2022), 137348.
H. Mantysaari, B.Schenke, C. Shen and W. Zhao, [arXiv:2208.00396 [hep-ph]].

Probing protons at different resolutions

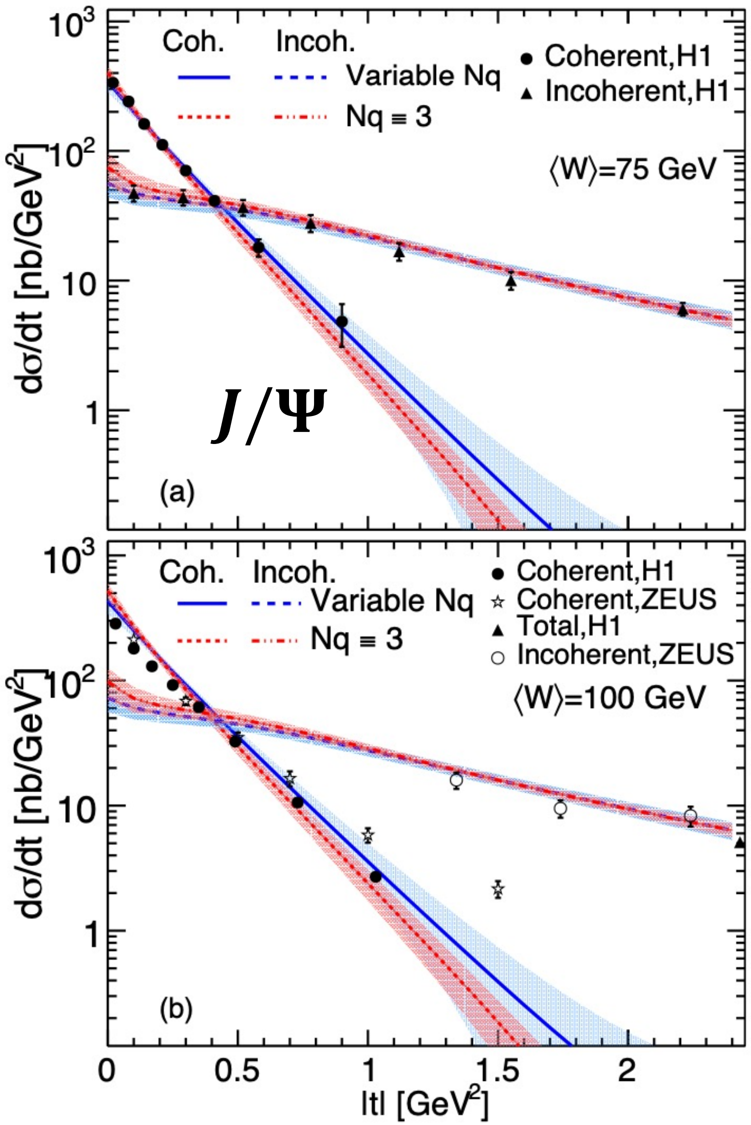

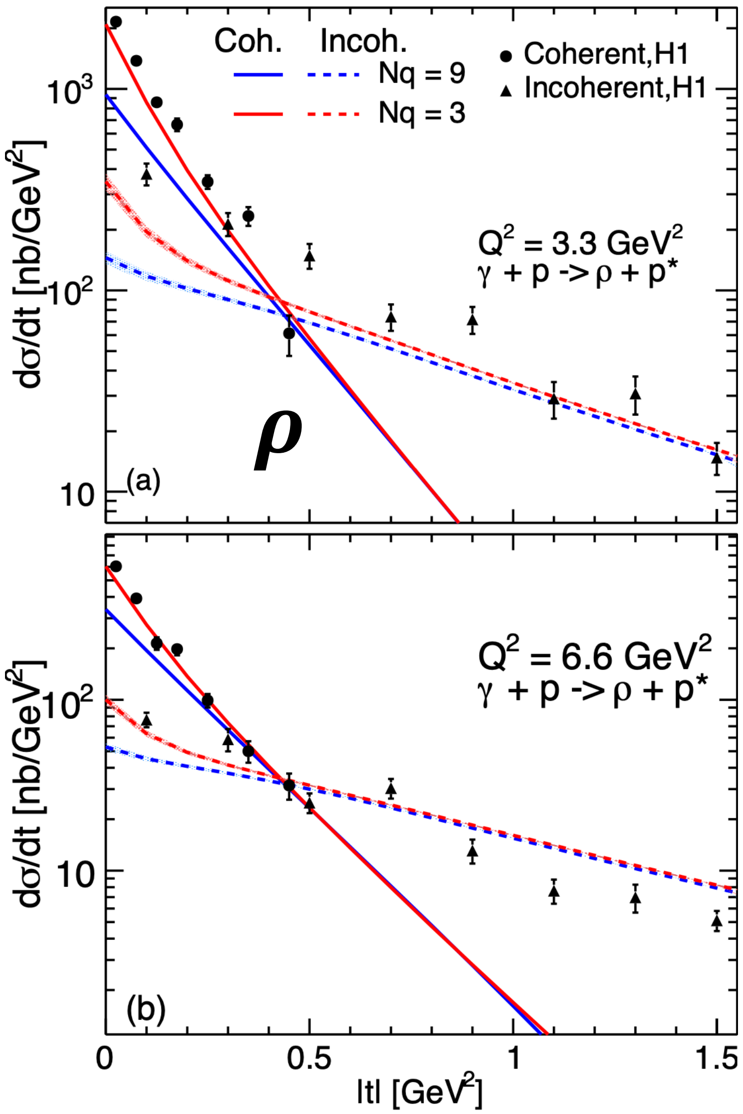

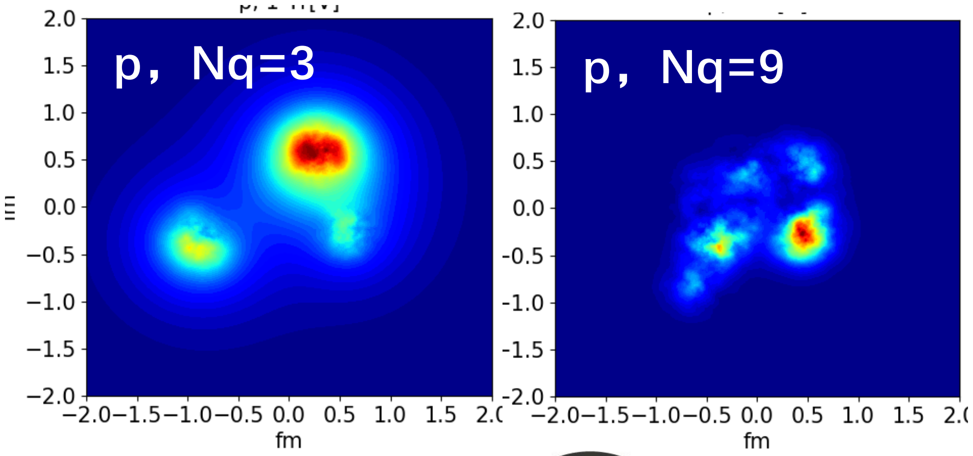

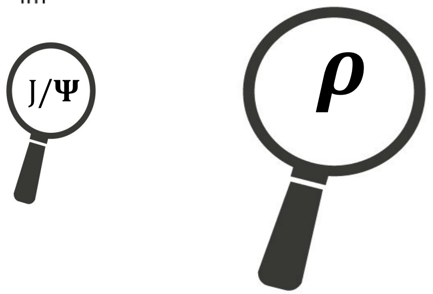

- The ρ mesons probe proton fluctuations at large length scales.
- Large differences observed for ρ productions between Nq=3 and Nq=9 MAPs.

H. Mantysaari, B.Schenke, C. Shen and W. Zhao, Phys. Lett. B 833 (2022), 137348, and in progress.

Connecting to Relativistic Nuclear Collisions

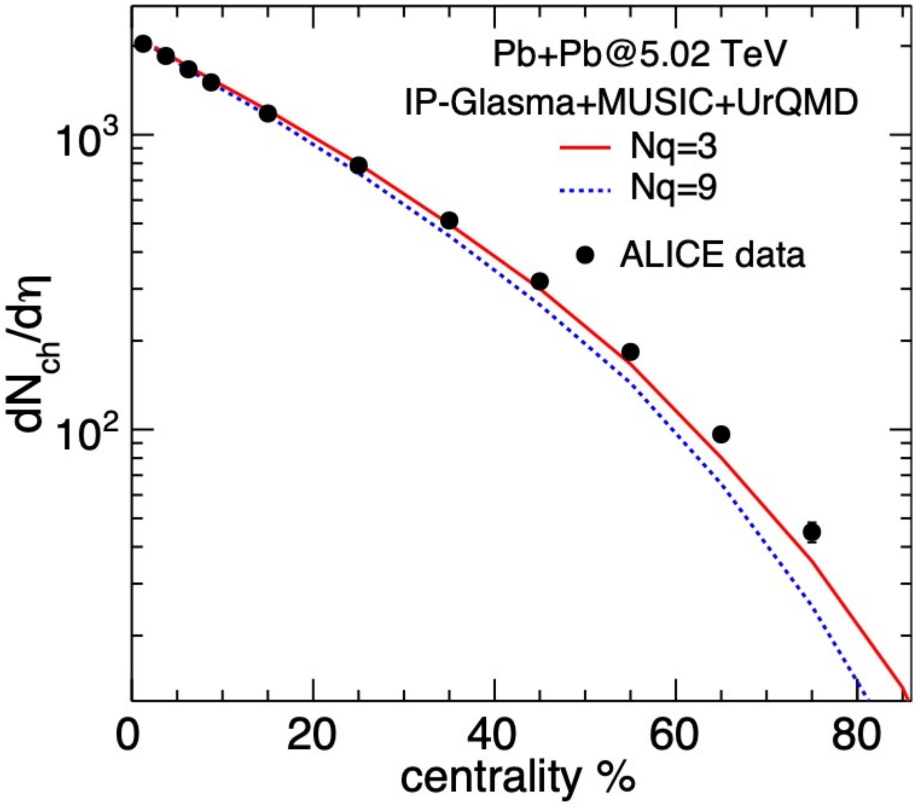

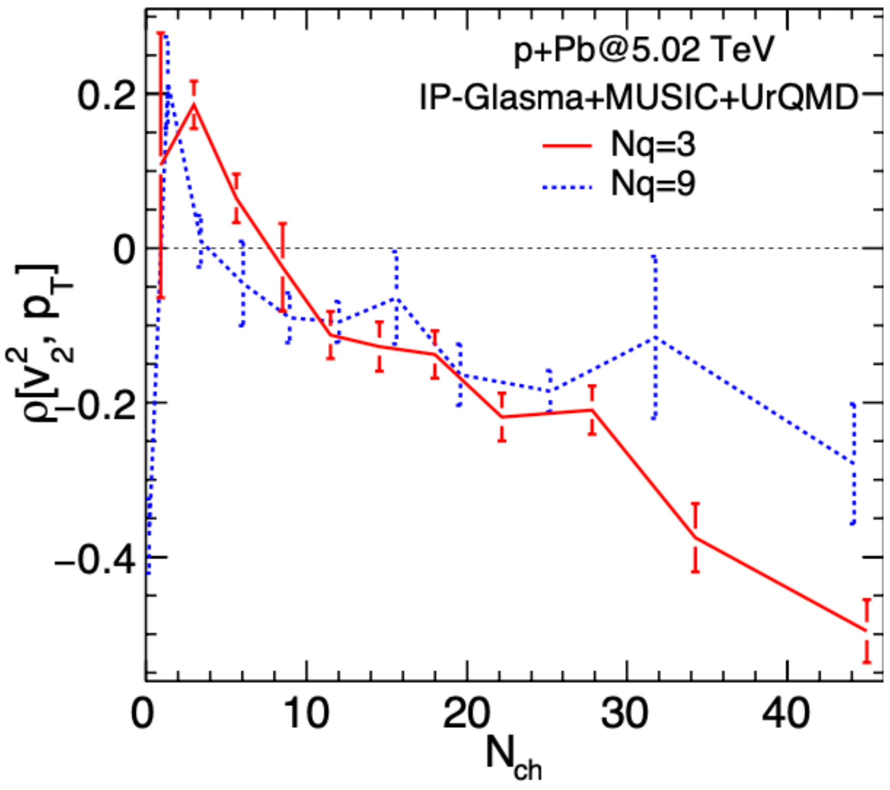

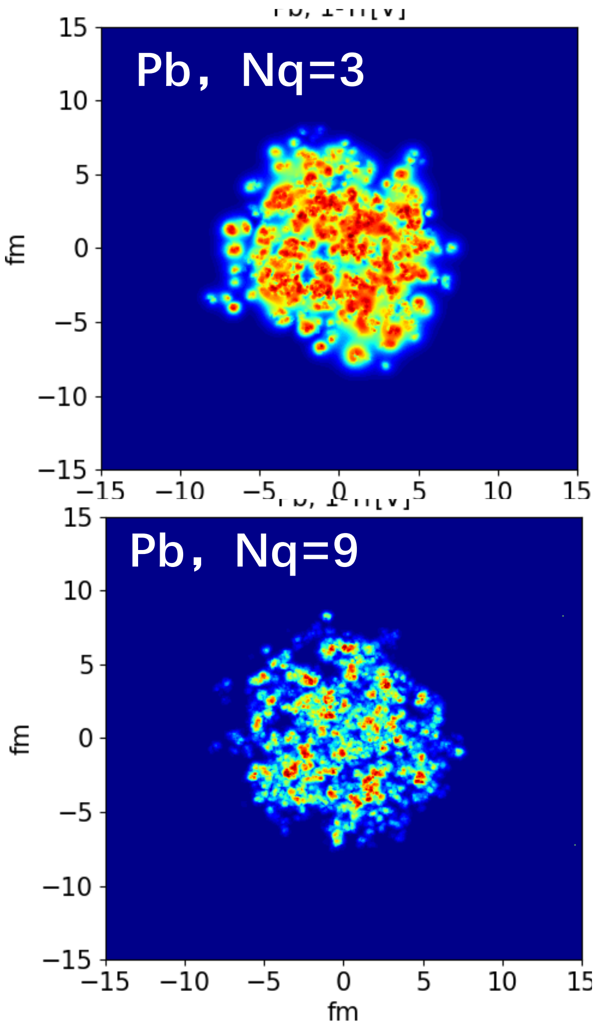

- Pb+Pb $dN_{ch}/d\eta$ data favors the small Nq case.
- $v_2 - p_T$ correlator in p+Pb is a promising observable.
- We would like to explore more experimental constraints using HERA + LHC Pb+Pb and p+Pb data

H.Mantysaari, B.Schenke, C. Shen and W. Zhao, Phys. Lett. B 833 (2022), 137348.
H.Mantysaari, B.Schenke, C. Shen and W. Zhao, [arXiv:2208.00396 [hep-ph]].

Accessing nuclear deformation at small x

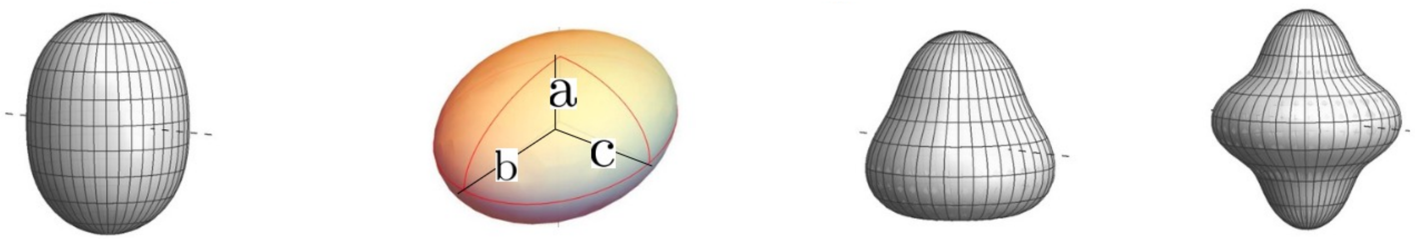

Nuclear structure

Generalized Woods-Saxon profile

$$\rho(r,\Theta,\Phi) \propto \frac{1}{1+\exp\left([r-R(\Theta,\Phi)]/a\right)}\ , \quad R(\Theta,\Phi) = R_0\left[1+\beta_2\left(\cos\gamma Y_{20}(\Theta)+\sin\gamma Y_{22}(\Theta,\Phi)\right)+\beta_3 Y_{30}(\Theta)+\beta_4 Y_{40}(\Theta)\right]$$

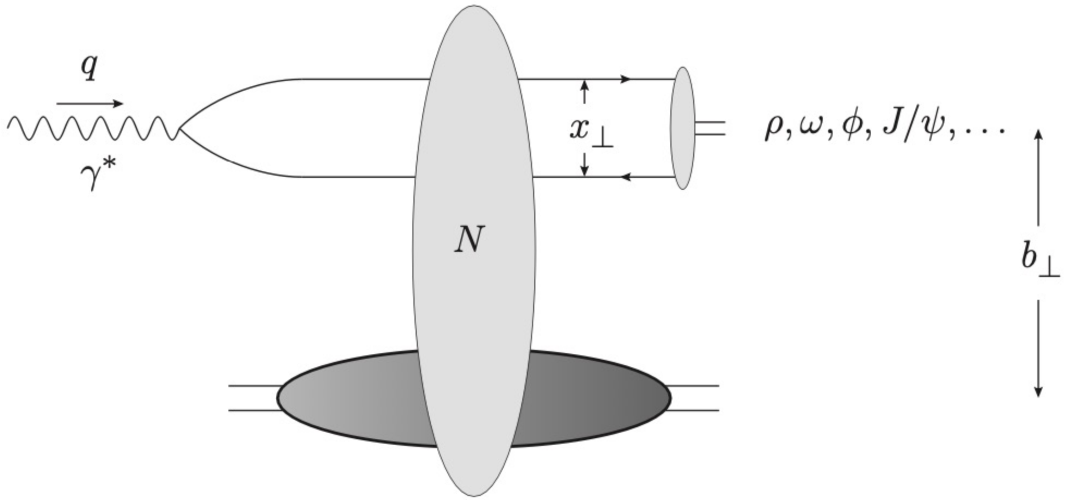

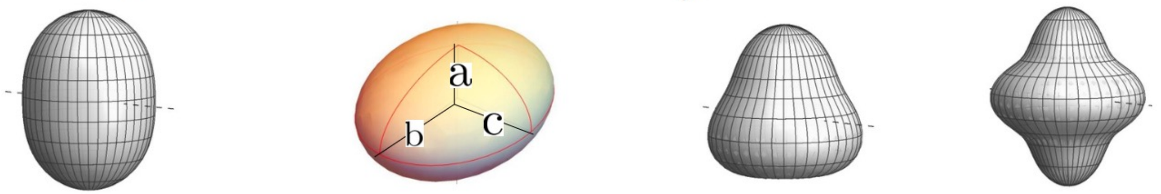

Taken from Giuliano’ s slide

- Sample nucleon positions based on the Wood—Saxon distribution.
- Different deformation parameters controls the geometric deformation at different length scale.
- Probe the nuclear geometric deformation (deformed gluon density distributions) by the diffractive process.

γ^* + U → J/ψ + U*

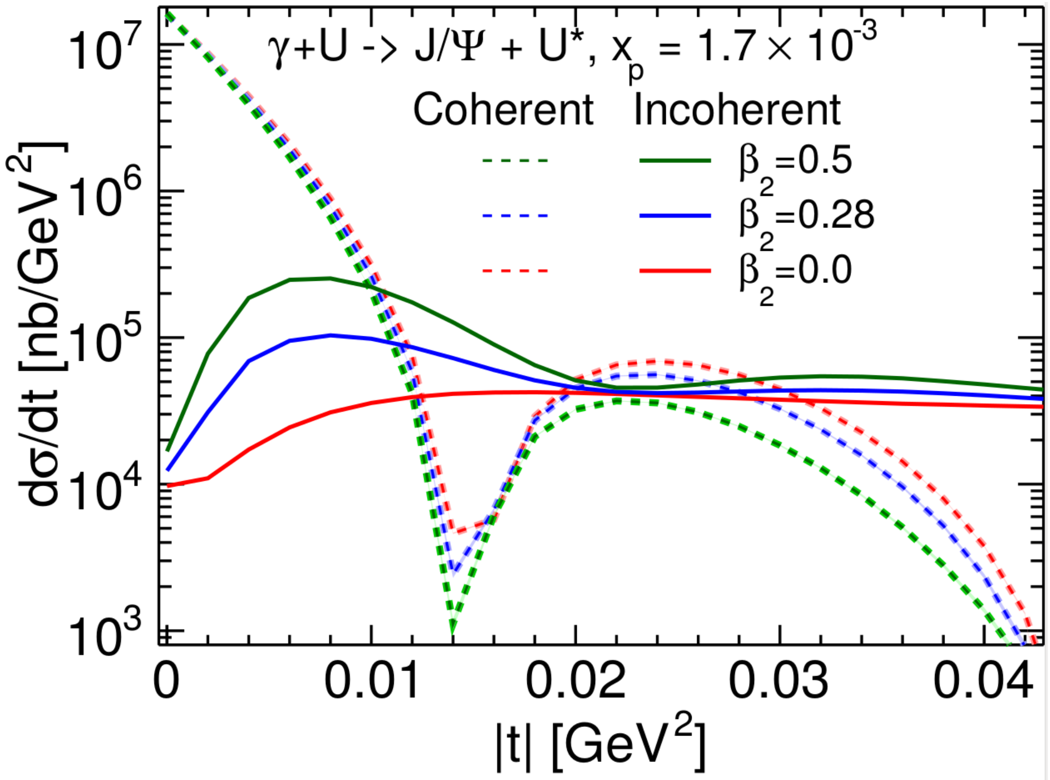

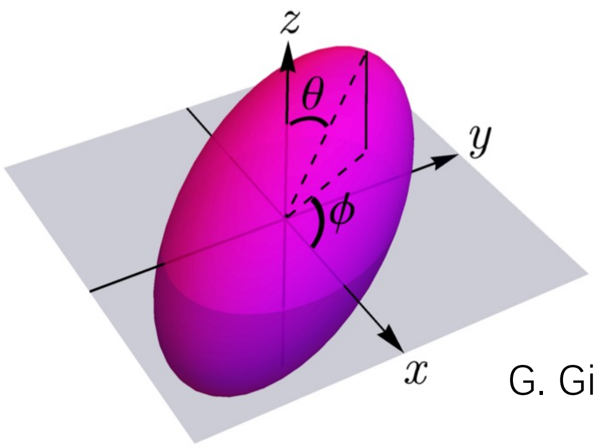

G. Giacalone, arXiv: 2004.14463

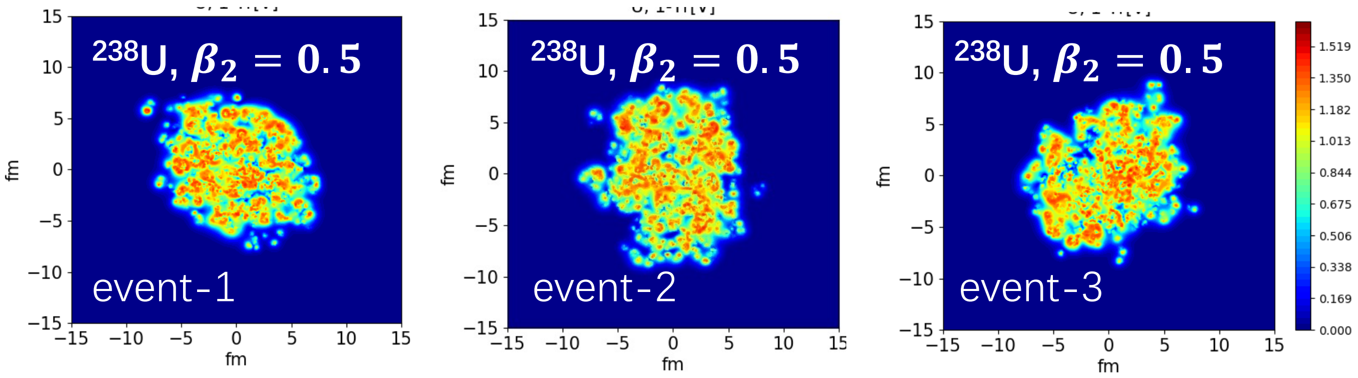

- With $\beta > 0$, the configurations projected onto x-y plane have great fluctuations.
- β_2 quadrupole deformation of the nucleus affects incoherent cross section at small|t|(large length scales) and provides direct information on the nuclear structure at small x.

H.Mantysaari, B.Schenke, C. Shen and W. Zhao, [arXiv:2303.04866].

Multi-scale imaging (β_2, β_3, and β_4)

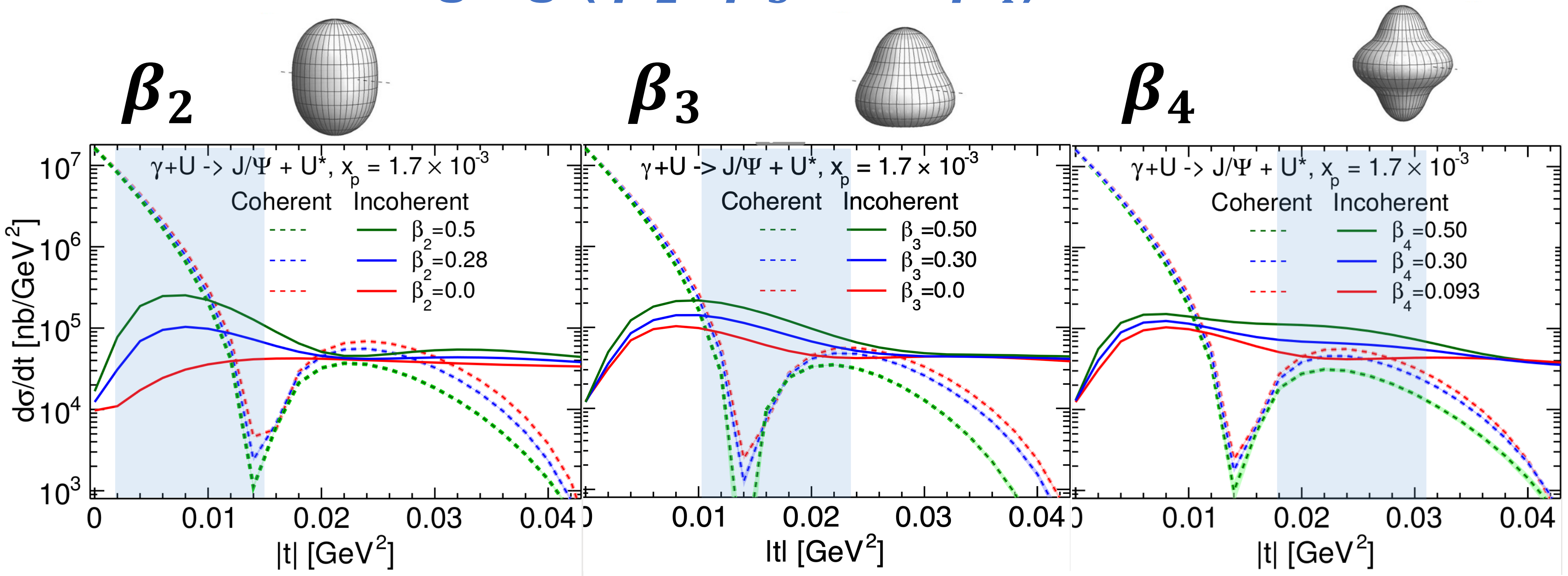

- β_2 , β_3 and β_4 manifest themselves at different |t| regions (different length scales).
- In the future, we will train the emulator with diffractive results. Then use trained emulator to predict the Woods-Saxon deformation parameters.

H.Mantysaari, B.Schenke, C. Shen and W. Zhao, [arXiv:2303.04866].

"See" sub-nucleon structures

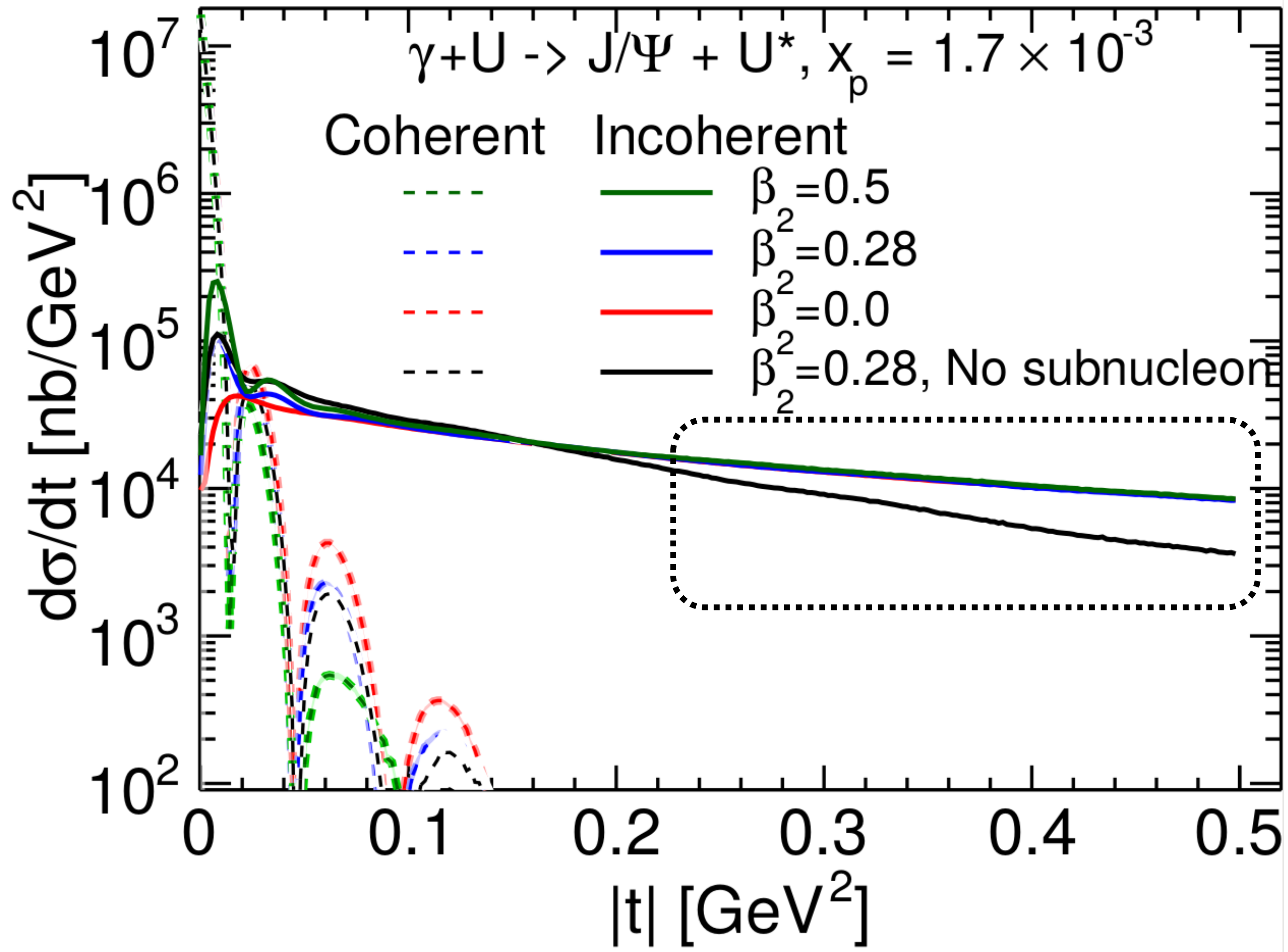

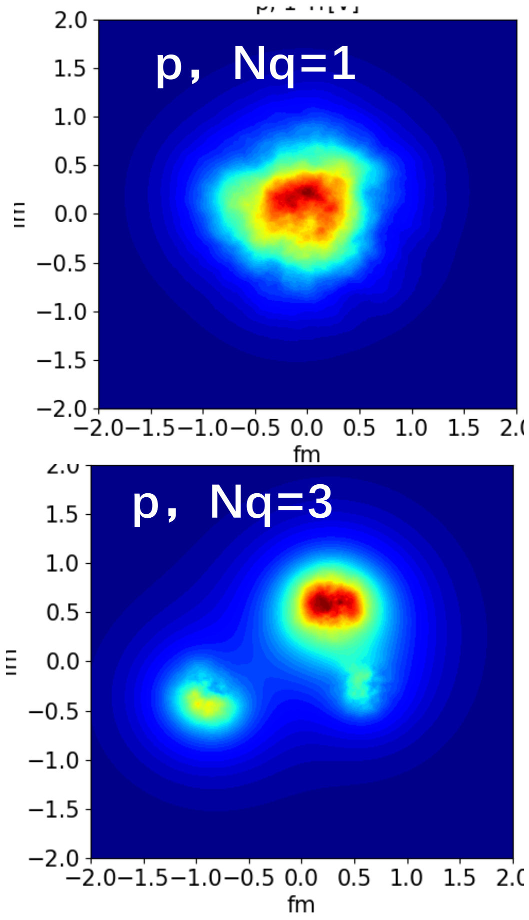

- High |t| region of $\gamma^* + A$ incoherent cross section probes sub-nucleon structures.

H.Mantysaari, B.Schenke, C. Shen and W. Zhao, Phys. Lett. B 833 (2022), 137348.
H.Mantysaari, B.Schenke, C. Shen and W. Zhao, [arXiv:2303.04866].

JIMWLK evolution to smaller xp

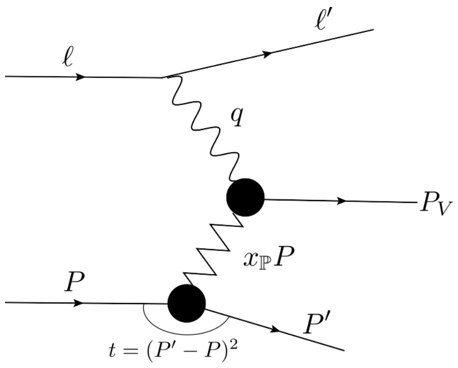

$$x_{\mathbb{P}} \equiv \frac{(P - P')\cdot q}{P\cdot q}$$

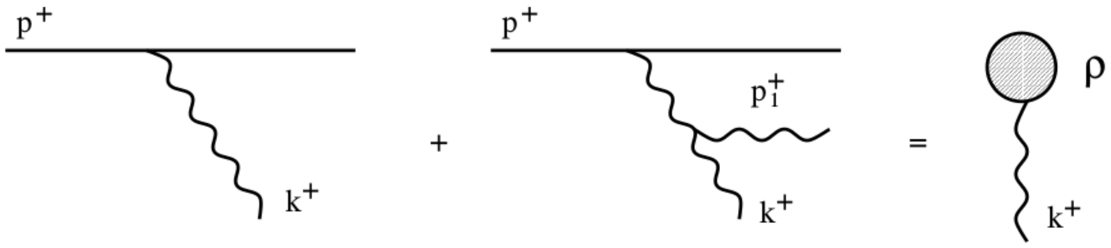

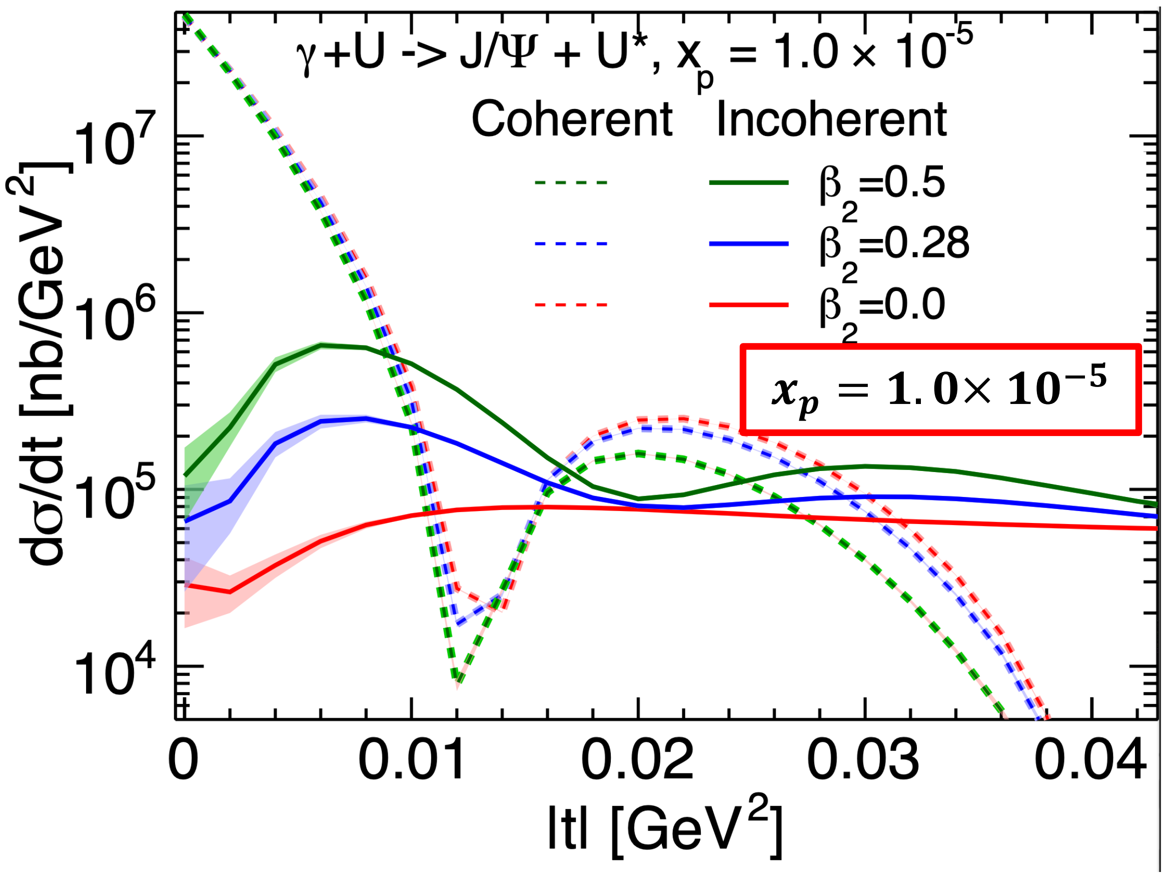

JIMWLK evolution:
absorb quantum fluctuations at intermediate x range as the color sources of smaller x.

- JIMWLK evolution doesn't wash out this effects.

H.Mantysaari, B.Schenke, C. Shen and W. Zhao [arXiv:2303.04866]..
H.Mantysaari, B.Schenke PRD, 98, 034013.
T. Lappi and H. Mantysaari, EPJC 73, 2307 (2013).
Yuri V. Kovchegov, QUANTUM CHROMODYNAMICS A T HIGH ENERGY

JIMWLK evolution to smaller xp

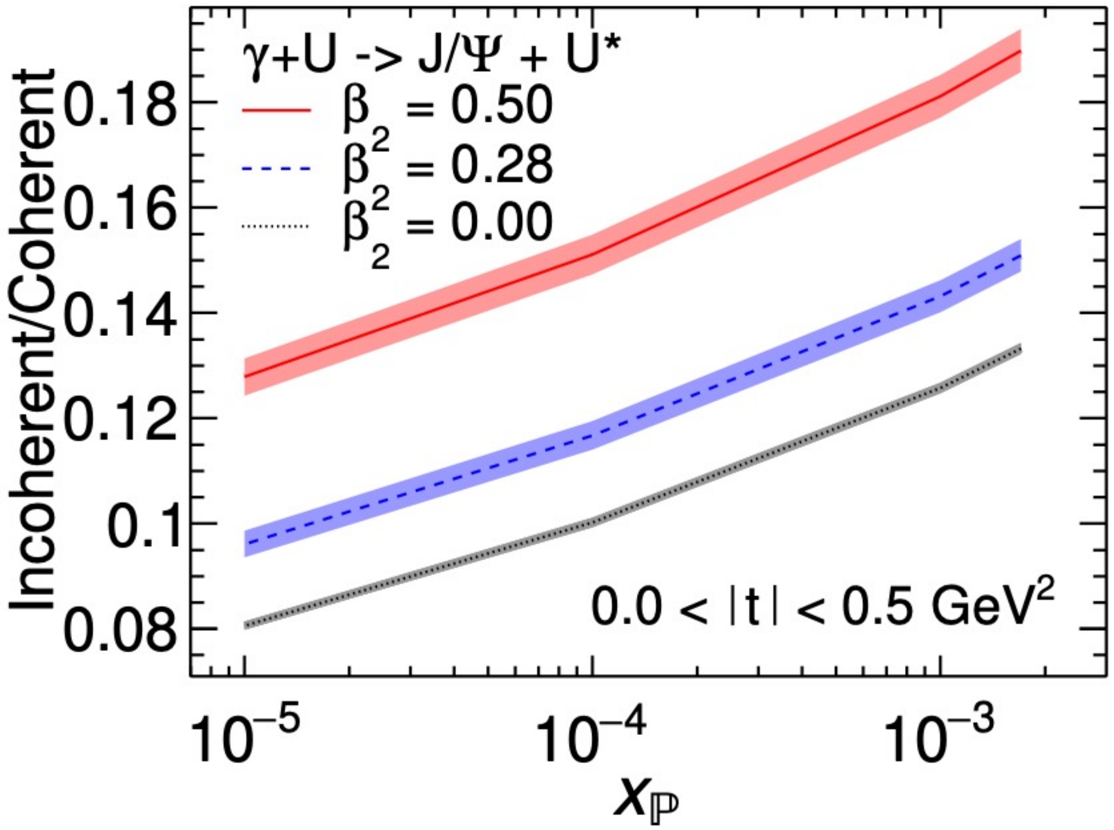

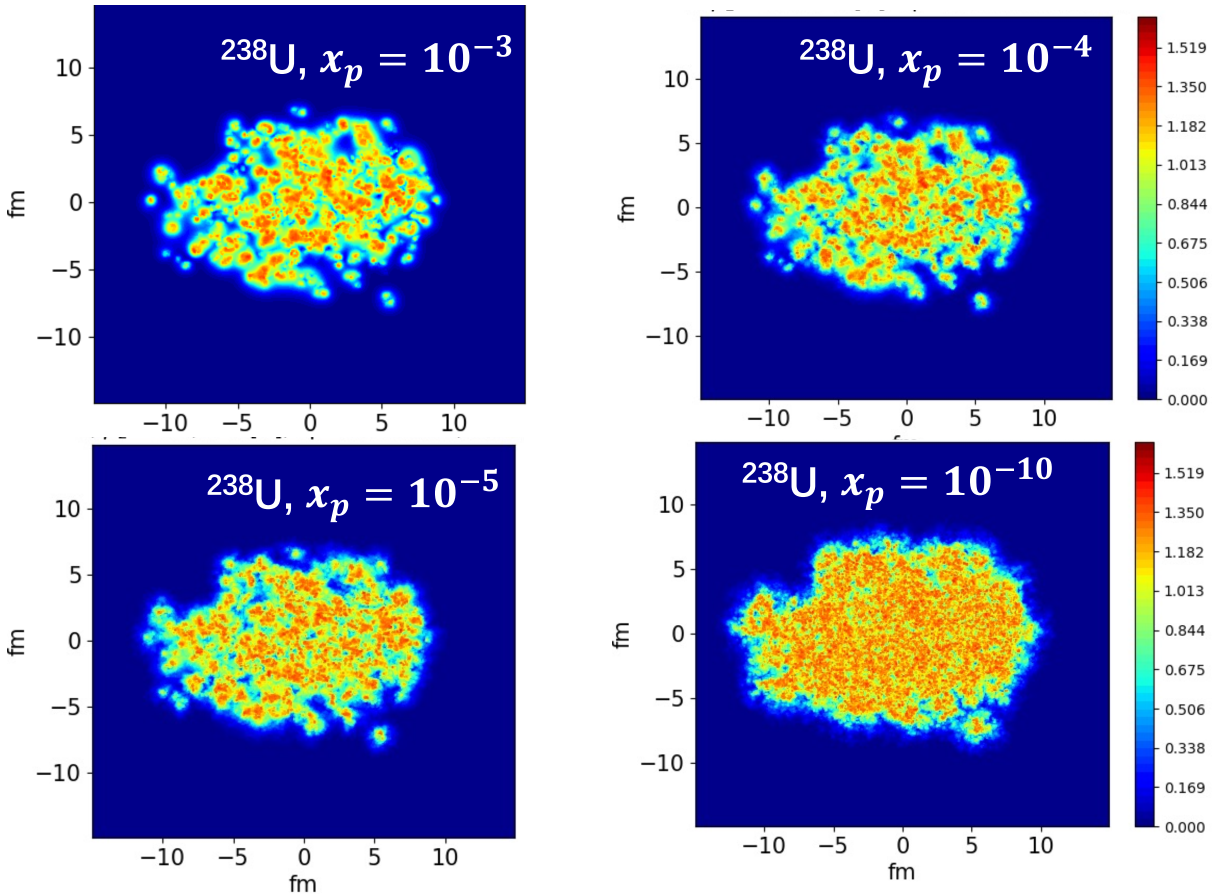

- Incoherent-to-coherent ratio effectively suppresses model uncertainties from wave functions.
- At smaller x_p, nucleon is smoother, reduces the fluctuations, decreases Incoherent-to-coherent ratio.
- JIMWLK evolution doesn't wash out difference between different β_2 (β_2 controls overall shape).

H.Mantysaari, B.Schenke, C. Shen and W. Zhao, [arXiv:2303.04866].
H.Mantysaari, B.Schenke PRD, 98, 034013.

Probing ^{20}Ne and ^{16}O

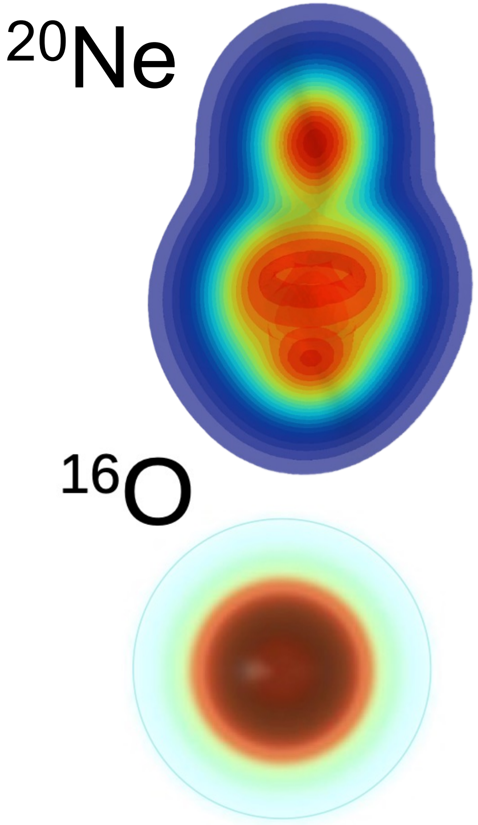

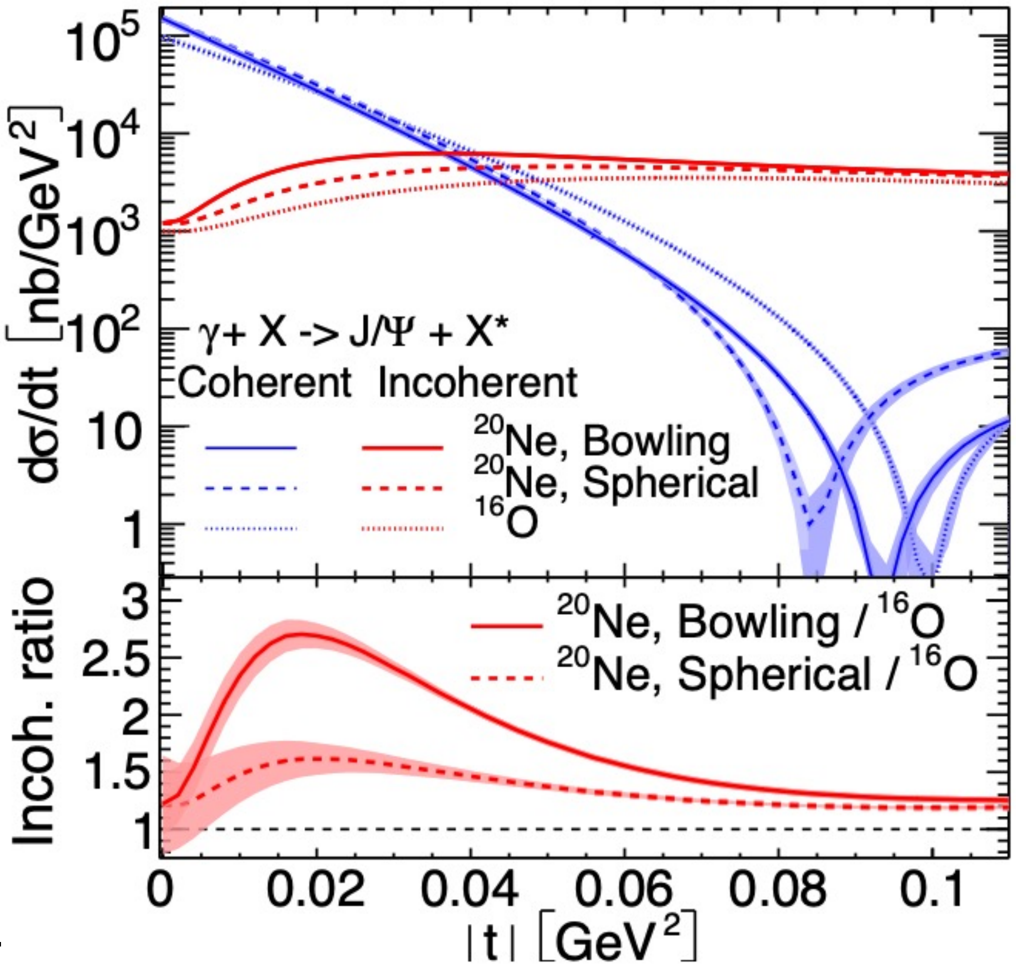

Nucleon density distribution is taken from G. Giacalone.

- Incoherent cross section at small |t| captures the deformation of the ^{20}Ne.
- Significant difference between ^{20}Ne and ^{16}O diffractive cross sections is observed.

H.Mantysaari, B.Schenke, C. Shen and W. Zhao, [arXiv:2303.04866].

Summary

- We perform the first Bayesian analysis to constrain the proton shape fluctuations from diffractive J/Ψ data at HERA.
- Diffractive vector meson production can "see" the nuclear shape and fluctuations at different scales!
- JIMWLK evolution doesn't wash out this effect.

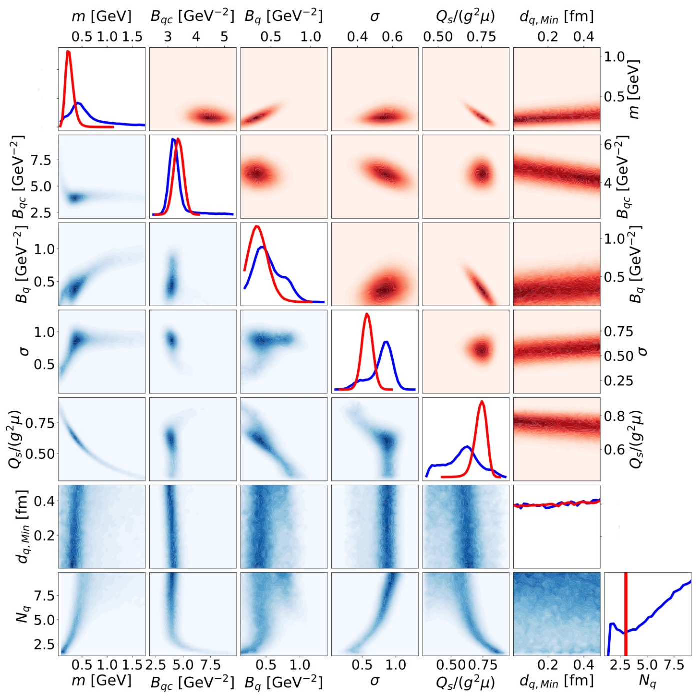

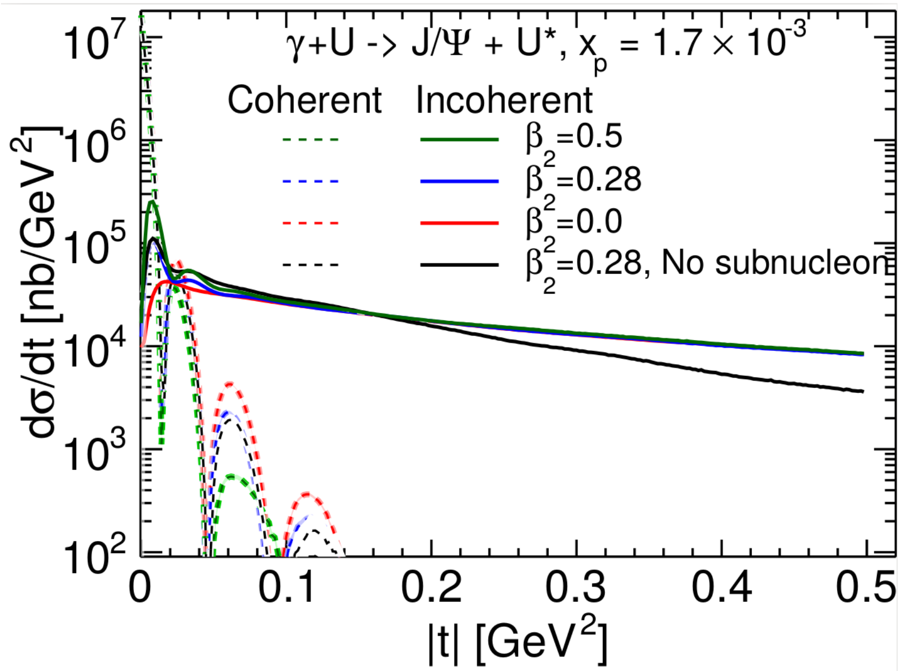

Thanks for Your Attentions!

Back Up

Dipole-target scattering amplitude (CGC)

- The dipole amplitude N can be calculated from Wilson line V(x)

$$N\left(\mathbf{b}=\frac{\mathbf{x}+\mathbf{y}}{2},\mathbf{r}=\mathbf{x}-\mathbf{y},x_{\mathbb{P}}\right)=1-\frac{1}{N_c}\mathrm{Tr}\left(V(\mathbf{x})V^\dagger(\mathbf{y})\right). \quad V(\mathbf{x})=P\exp\left(-ig\int dx^-\frac{\rho(x^-,\mathbf{x})}{\nabla^2+m^2}\right)$$

- Using MV model for Gaussian distribution of color charge ρ:

$$\langle\rho^a(\mathbf{b}_\perp)\rho^b(\mathbf{x}_\perp)\rangle = g^2\mu^2(x,\mathbf{b}_\perp)\delta^{ab}\delta^{(2)}(\mathbf{b}_\perp-\mathbf{x}_\perp)$$

Q_s: saturation scale, $Q_s/g^2\mu$ is a free parameter, Q_s is determined from IP-Sat parametrization.

- Or, equivalently, factorize $\mu(x,\mathbf{b}_\perp)\sim T(\mathbf{b}_\perp)\mu(x)$

N(r, x, b) accesses to the spatial structure of the target ($T_{p/A}$).

Schenke , etc.al. PhysRevLett.108.252301 , PhysRevC.86.034908, Mäntysaari, Schenke, 1603.04349;

Diffractive vector meson production

High energy factorization:

1. $\gamma^* \to q\bar{q}$ splitting, wave function $\Psi^{\gamma}(r, Q^2, z)$
2. $q\bar{q}$ dipole scatters elastically
3. $q\bar{q} \to J/\Psi$, wave function $\Psi^{V}(r, Q^2, z)$

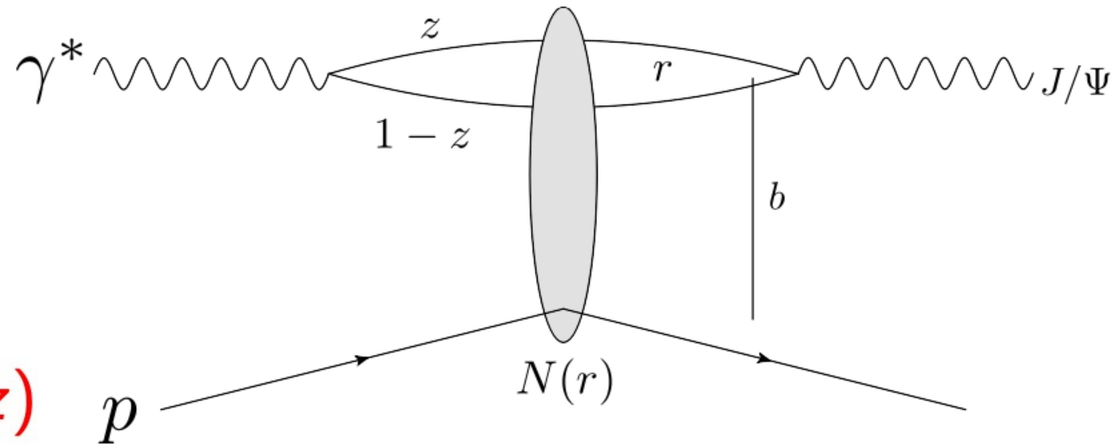

Diffractive scattering amplitude

Theoretically: no net color transfer

$$\mathcal{A}^{\gamma^* p \to Vp} \sim \int \mathrm{d}^2 b \mathrm{d}z \mathrm{d}^2 r \Psi^{\gamma *} \Psi^{V}(r, z, Q^2) \mathbf{e}^{-\mathrm{i}\mathbf{b}\cdot\mathbf{\Delta}} N(r, x, b)$$

Impact parameter, b, is the Fourier conjugate of the momentum transfer, $\Delta \approx \sqrt{-t}$

$N(\mathbf{r}_T, \mathbf{b}_T, x) = 1 - \exp\left(-\mathbf{r}_T{}^2 F(\mathbf{r}_T, x) T_p(\mathbf{b}_T)\right)$ **accesses to the spatial structure ($\boldsymbol{T_{p/A}}$)**

$F(\mathbf{r}_T, x) = \frac{\pi^2}{2N_c} \alpha_s(\mu^2) x g(x, \mu^2)$. $xg(x, \mu^2)$, gluon density at x and scale μ^2 $(\mu^2 \sim \mu_0^2 + 1/r_T^2)$.

Miettinen, Pumplin, PRD 18, 1978; Caldwell, Kowalski, 0909.1254; Mäntysaari, Schenke, 1603.04349; Mäntysaari, 2001.10705

Probing isobar, Ru/Zr

system to run	R_0 (fm)	a_0 (fm)	β_2	β_3	γ (°)	dmin(fm)
Case1 (^{96}Ru+^{96}Ru) [full ^{96}Ru]	5.09	0.46	0.16	0	30	0.0
Case2 (^{96}Ru+^{96}Ru)	5.09	0.46	0.16	0	0	0.9
Case3 (^{96}Ru+^{96}Ru)	5.09	0.46	0.16	0.20	0	0.9
Case4 (^{96}Ru+^{96}Ru)	5.09	0.46	0.06	0.20	0	0.9
Case5 (^{96}Ru+^{96}Ru)	5.09	0.52	0.06	0.20	0	0.9
Case6 (^{96}Zr+^{96}Zr) [full ^{96}Zr]	5.02	0.52	0.06	0.20	0	0.9

$$R(\Theta,\Phi) = R_0\left[1+\beta_2\Big(\cos\gamma Y_{20}(\Theta)+\sin\gamma Y_{22}(\Theta,\Phi)\Big)+\beta_3 Y_{30}(\Theta)+\beta_4 Y_{40}(\Theta)\right]$$

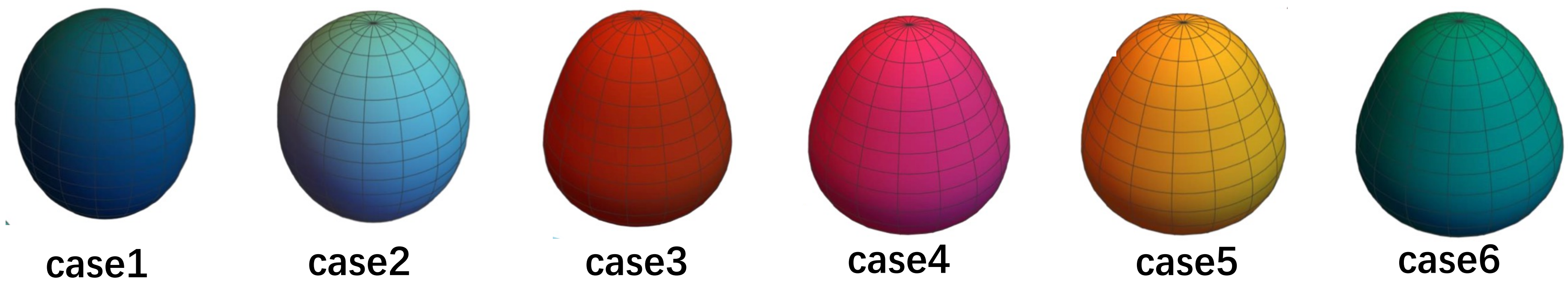

Taken from Willian Matioli Serenone's slide.

- Impose a minimal distance, dmin, between nucleons.
- When a nucleon is added and violates the minimum distance criterion with one or more already sampled nucleons, we resample its azimuthal angle ϕ to keep the distributions of radial distances and polar angles unchanged. ($\gamma \neq 0$, dmin = 0.0 fm)

J. S. Moreland, J. E. Bernhard and S. A. Bass, Phys. Rev. C 92 (2015) no.1, 011901.

Probing isobar, Ru/Zr

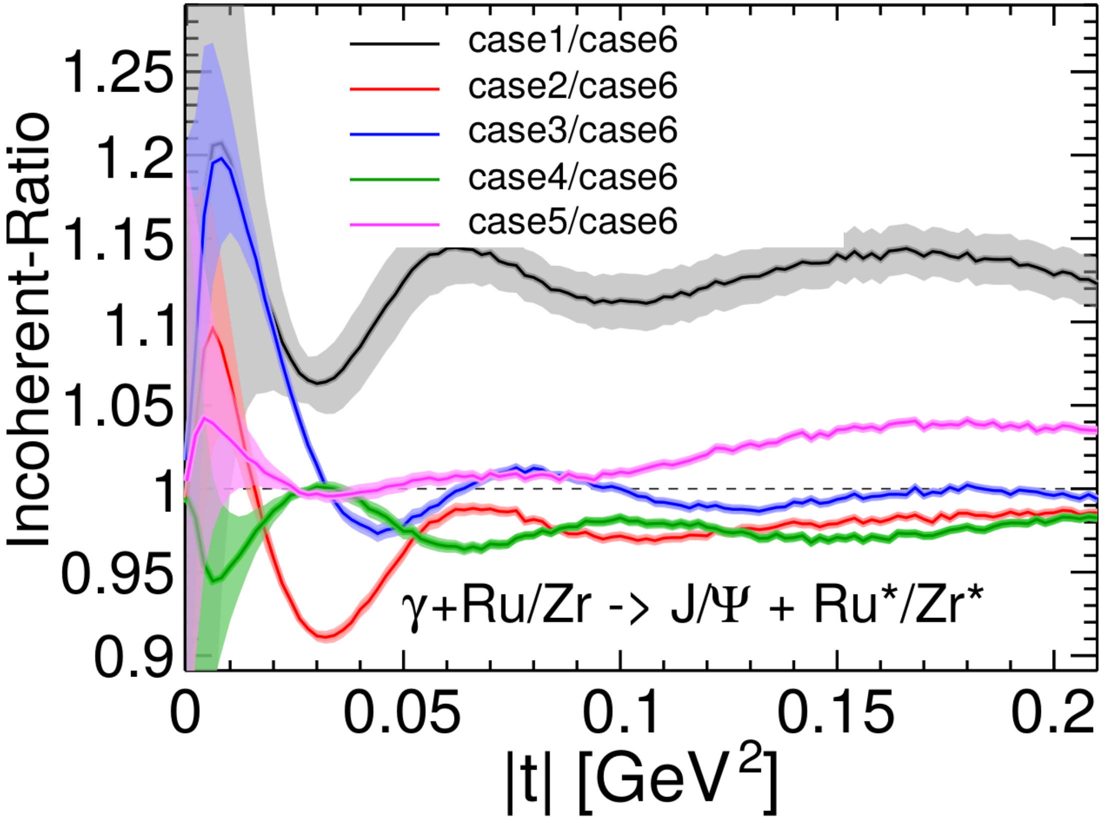

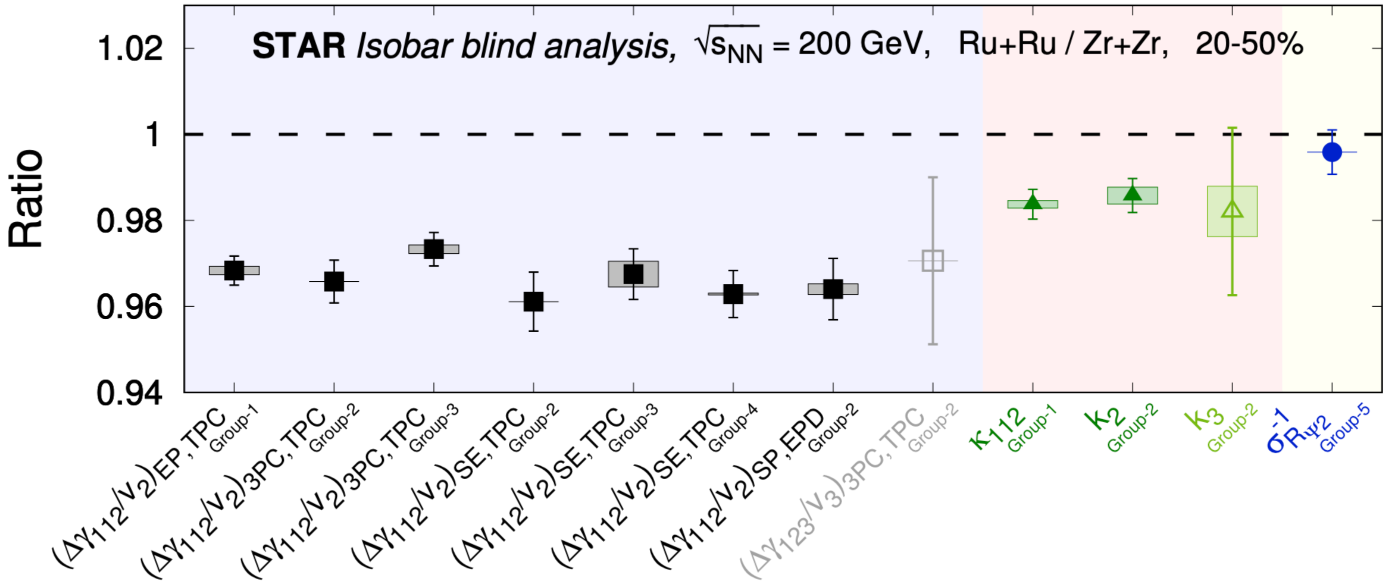

STAR, Phys. Rev. C 105 (2022) no.1, 014901.

- Differences of incoherent J/Ψ productions cross section between case2 -- case6 are within 5%.
- The difference between case1 and others mainly comes from dmin.

H.Mantysaari, B.Schenke, C. Shen and W. Zhao, in progress.

MAP

Parameter	Description	$N_q = 9$	$N_q = 3$
m [GeV]	Infrared regulator	0.780	0.246
B_{qc} [GeV^{-2}]	Proton size	3.98	4.45
B_q [GeV^{-2}]	Hot spot size	0.594	0.346
σ	Magnitude of Q_s fluctuations	0.932	0.563
$Q_s/(g^2\mu)$	$Q_s \Rightarrow$ color charge density	0.492	0.747
$d_{q,\mathrm{Min}}$ [fm]	Min hot spot distance	0.265	0.254
N_q	Number of hot spots	3	9
S	Hydro normalization	0.1135	0.235

JIMWLK

$$V_{ij}(\vec{x}_T) = \mathscr{P}\left(ig \int_{-\infty}^{\infty} A^{+,c}(z^-, \vec{x}_T)\, t^c_{ij}\, dz^- \right)$$

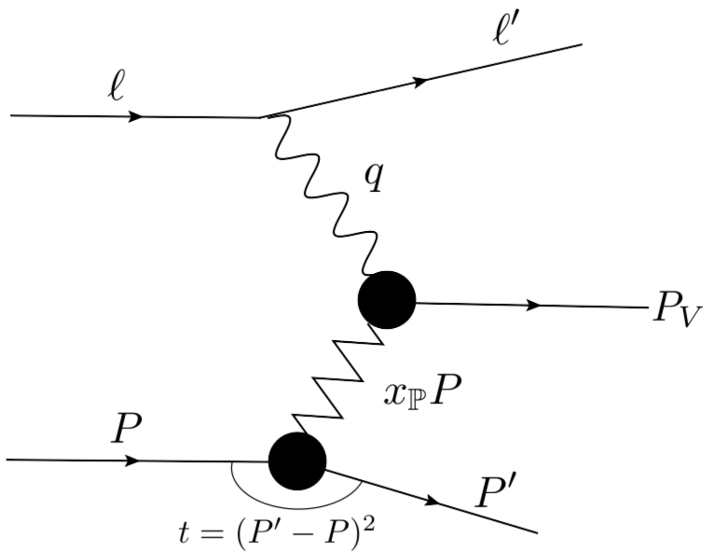

Evolve the Wilson lines according to the Langevin equation

$$\frac{\mathrm{d}}{\mathrm{d}y} V_{\mathbf{x}} = V_{\mathbf{x}}(it^a)\left[\int \mathrm{d}^2\mathbf{z}\, \varepsilon^{ab,i}_{\mathbf{x},\mathbf{z}}\, \xi_{\mathbf{z}}(y)^b_i + \sigma^a_{\mathbf{x}}\right].$$

The deterministic drift term is

$$\sigma^a_{\mathbf{x}} = -i\frac{\alpha_s}{2\pi^2}\int \mathrm{d}^2\mathbf{z}\, S_{\mathbf{x}-\mathbf{z}}\mathrm{Tr}[T^a U^\dagger_{\mathbf{x}} U_{\mathbf{z}}], \quad S_{\mathbf{x}} = 1/\mathbf{x}^2$$

The random noise is Gaussian and local in coordinates, color, and rapidity with expectation value zero and

$$\langle \xi^a_{\mathbf{x},i}(y)\xi^b_{\mathbf{y},j}(y')\rangle = \delta^{ab}\delta^{ij}\delta^{(2)}_{\mathbf{xy}}\delta(y-y').$$

The coefficient of the noise in the stochastic term is

$$\varepsilon^{ab,i}_{\mathbf{x},\mathbf{z}} = \left(\frac{\alpha_s}{\pi}\right)^{1/2} K^i_{\mathbf{x}-\mathbf{z}}[1 - U^\dagger_{\mathbf{x}} U_{\mathbf{z}}]^{ab}, \qquad K^i_{\mathbf{x}} = \frac{x^i}{\mathbf{x}^2}.$$

H.Mantysaari, B.Schenke PRD, 98, 034013.

JIMWLK

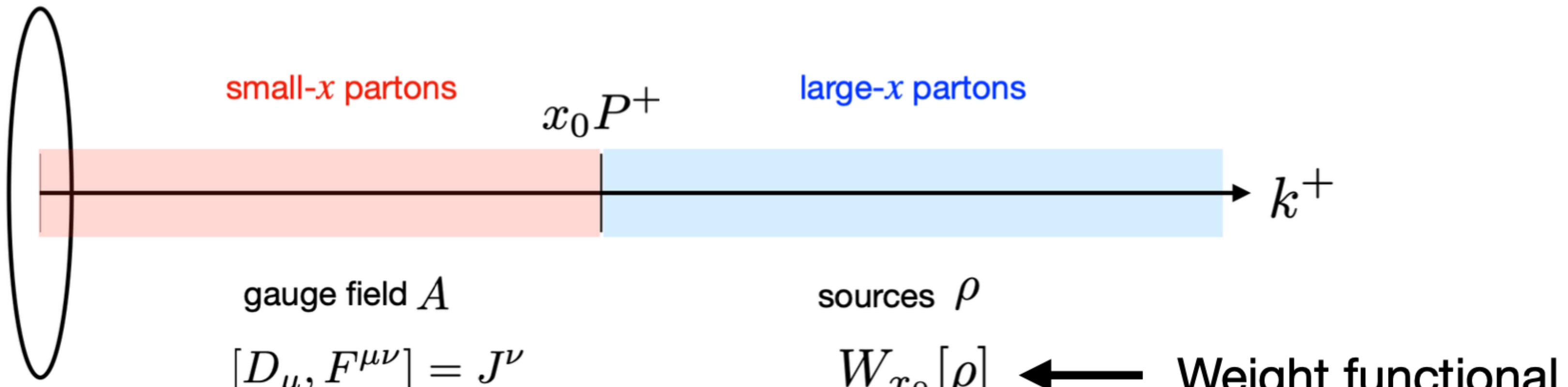

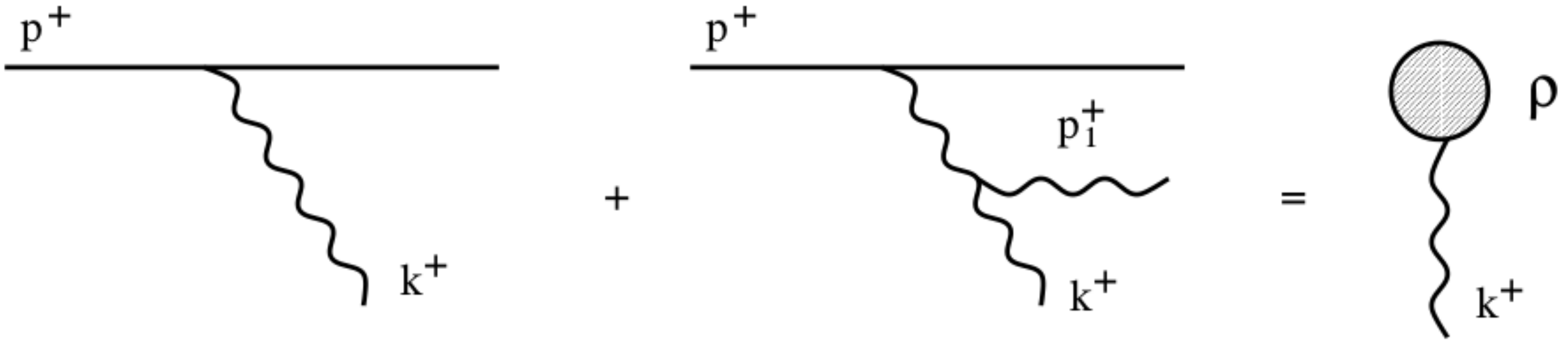

$$\frac{\partial W_\tau[\alpha]}{\partial \tau} = \frac{1}{2}\int_{\boldsymbol{x},\boldsymbol{y}} \frac{\delta^2}{\delta\alpha_\tau^a(\boldsymbol{x})\delta\alpha_\tau^b(\boldsymbol{y})}\left[W_\tau \chi_{xy}^{ab}\right] - \int_{\boldsymbol{x}} \frac{\delta}{\delta\alpha_\tau^a(\boldsymbol{x})}\left[W_\tau \sigma_x^a\right],$$

Wilson lines

$$V_{ij}(\vec{x}_T) = \mathcal{P}\left(ig \int_{-\infty}^{\infty} A^{+,c}(z^-,\vec{x}_T)\, t^c_{ij}\, dz^- \right)$$

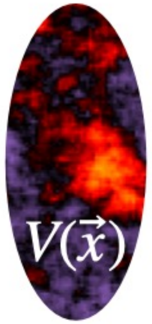

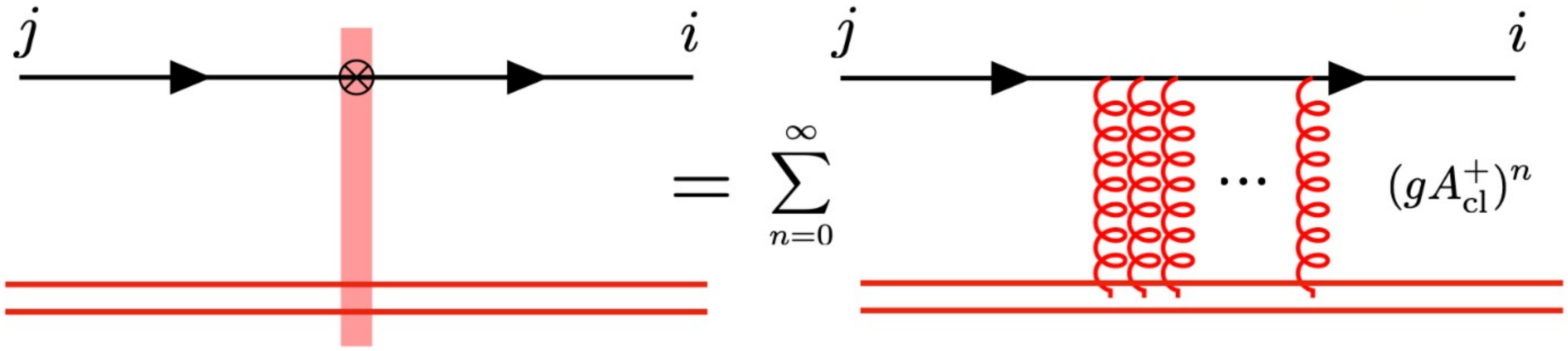

MULTIPLE INTERACTIONS NEED TO BE RESUMMED, BECAUSE $A^+ \sim 1/g$

Wilson lines

$$\mathcal{A}^{\gamma^* p \to Vp} \sim \int \mathrm{d}^2 b \mathrm{d}z \mathrm{d}^2 r \Psi^{\gamma^*} \Psi^V (r, z, Q^2) \mathbf{e}^{-i\mathbf{b}\cdot\mathbf{\Delta}} N(r, x, b)$$

$$N_\Omega(\mathbf{r}_\perp, \mathbf{b}_\perp, x_\mathbb{P}) = 1 - \frac{1}{N_c} \mathrm{tr}\left[V\left(\mathbf{b}_\perp + \frac{\mathbf{r}_\perp}{2}\right) V^\dagger\left(\mathbf{b}_\perp - \frac{\mathbf{r}_\perp}{2}\right)\right].$$

$$V(\mathbf{x}_\perp) = \mathrm{P}_- \left\{ \exp\left(-ig \int_{-\infty}^{\infty} \mathrm{d}z^- \frac{\rho^a(x^-, \mathbf{x}_\perp) t^a}{\boldsymbol{\nabla}^2 - m^2} \right) \right\}$$

$$g^2 \langle \rho^a(x^-, \mathbf{x}_\perp) \rho^b(y^-, \mathbf{y}_\perp) \rangle = g^4 \lambda_A(x^-) \delta^{ab} \times \delta^{(2)}(\mathbf{x}_\perp - \mathbf{y}_\perp) \delta(x^- - y^-).$$

From the dipole amplitude $\mathcal{N}(x, \mathbf{r}_\perp, \mathbf{b}_\perp) = (d\sigma^p_{\rm dip}/d^2\mathbf{b}_\perp)(x, \mathbf{r}_\perp, \mathbf{b}_\perp)/2$ given by Eq. (1), we can extract a saturation scale $Q_s(x)$ by using the definition that $Q_s^2 = 2/R_s^2$, with R_s defined via $\mathcal{N}(x, R_s) = 1 - \exp(-1/2)$. Note that $\mathcal{N}$ and Q_s also depend on the thickness function T_A

$$\mu^2 = \int \mathrm{d}x^- \lambda_A(x^-), \qquad \frac{Q_s(\mathbf{x}_\perp)}{g^2 \mu},$$ is a free parameter

B. Schenke, C. Shen and P. Tribedy, Phys. Rev. C 102 (2020) no.4, 044905.
H.Mantysaari, B.Schenke, C. Shen and **W. Zhao**, Phys. Lett. B 833 (2022), 137348.

Universal Wilson lines

We use one framework to compute Wilson lines for a nucleus at a given energy.

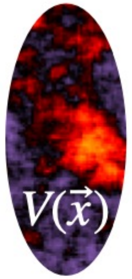

This allows to directly constrain parameters (like hot spot sizes) using one process (e.g. in e+A or e+p) and employ the model for another (e.g. in A+A or p+A)

e+A or UPC

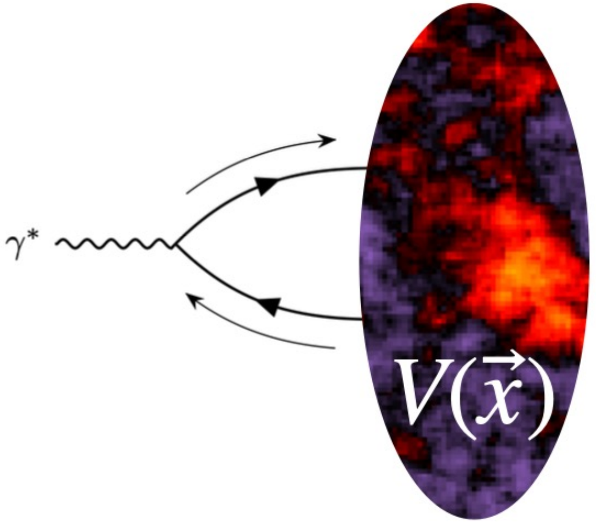

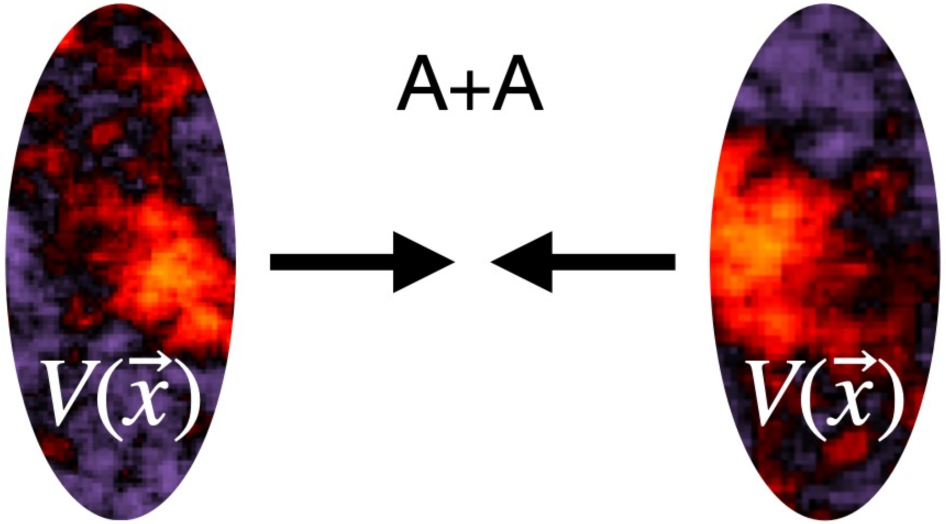

From Bjorn's slide

Color Glass Condensate (CGC): Sources and fields

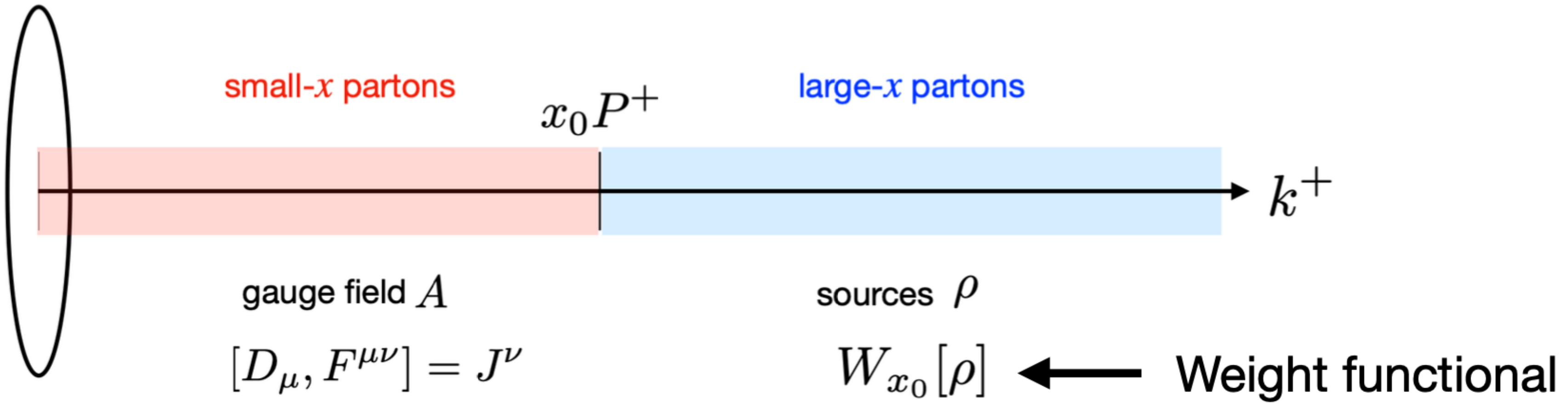

Two steps to compute expectation value of an observable $\mathcal{O}$:

1) Compute quantum expectation value $\mathcal{O}[\rho] = \langle \mathcal{O} \rangle_\rho$ for sources drawn from a given $W_{x_o}[\rho]$

2) Average over all possible configurations given the appropriate gauge invariant weight functional $W_{x_o}[\rho]$ (e.g. from McLerran Venugopalan model)

When $x \lesssim x_0$ the path integral $\langle \mathcal{O} \rangle_\rho$ is dominated by classical solution and we are done

For smaller x we need to do quantum evolution

4

From Bjorn's slide

Location of the first dip

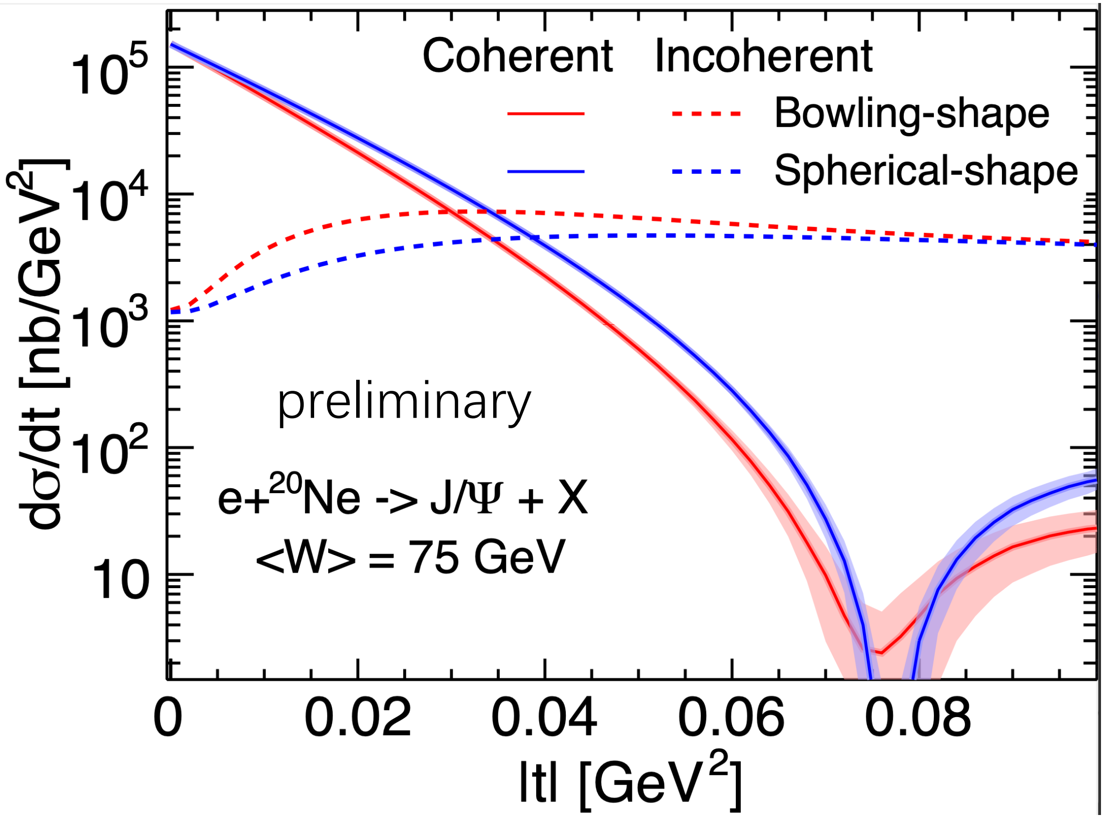

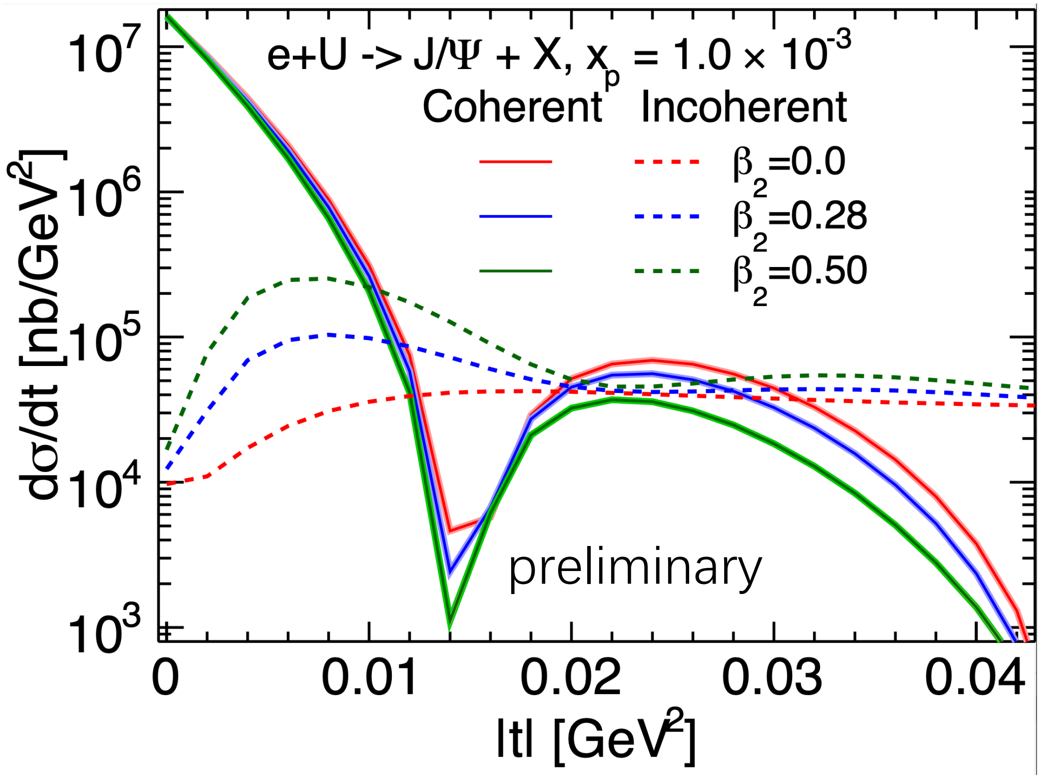

$$\frac{d\sigma^{\gamma^* p \to V p}}{dt} \sim e^{-B_p|t|}, \qquad T_p(\mathbf{b}_T) = \frac{1}{2\pi B_p} e^{-\mathbf{b}_T{}^2/(2B_p)}.$$

H.Mantysaari, B.Schenke, C. Shen and **W. Zhao**, in progress.

Wave functions

Forward photon wave functions (QED)

$$\Psi_{h\bar{h},\lambda=0}(r,z,Q) = e_f e\sqrt{N_c}\,\delta_{h,-\bar{h}}\,2Qz(1-z)\,\frac{K_0(\epsilon r)}{2\pi},$$

$$\Psi_{h\bar{h},\lambda=\pm1}(r,z,Q) = \pm e_f e\sqrt{2N_c}\,\{ie^{\pm i\theta_r}[z\delta_{h,\pm}\delta_{\bar{h},\mp} - (1-z)\delta_{h,\mp}\delta_{\bar{h},\pm}]\partial_r + m_f\delta_{h,\pm}\delta_{\bar{h},\pm}\}\,\frac{K_0(\epsilon r)}{2\pi},$$

Vector meson: Boosted Gaussian (Non-perturbative)

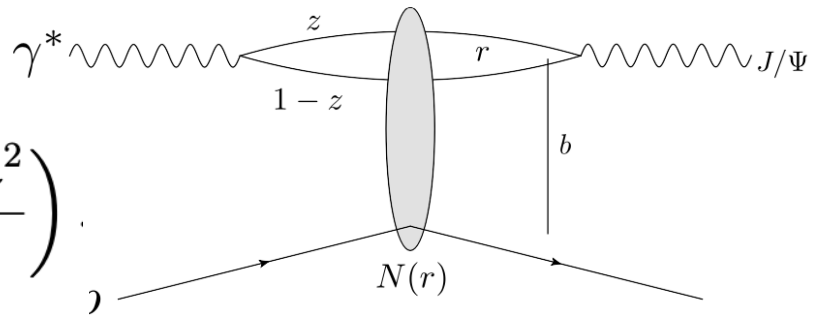

$$\phi_{T,L}(r,z) = \mathcal{N}_{T,L}\,z(1-z)\exp\left(-\frac{m_f^2\mathcal{R}^2}{8z(1-z)} - \frac{2z(1-z)r^2}{\mathcal{R}^2} + \frac{m_f^2\mathcal{R}^2}{2}\right)$$

Meson	M_V/GeV	f_V	m_f/GeV	$\mathcal{N}_T$	$\mathcal{N}_L$	$\mathcal{R}^2/\text{GeV}^{-2}$	$f_{V,T}$
J/ψ	3.097	0.274	1.4	0.578	0.575	2.3	0.307
ϕ	1.019	0.076	0.14	0.919	0.825	11.2	0.075
ρ	0.776	0.156	0.14	0.911	0.853	12.9	0.182

H. Kowalski, L. Motyka and G. Watt, Phys. Rev. D 74 (2006), 074016.

Different vector meson’s wave functions

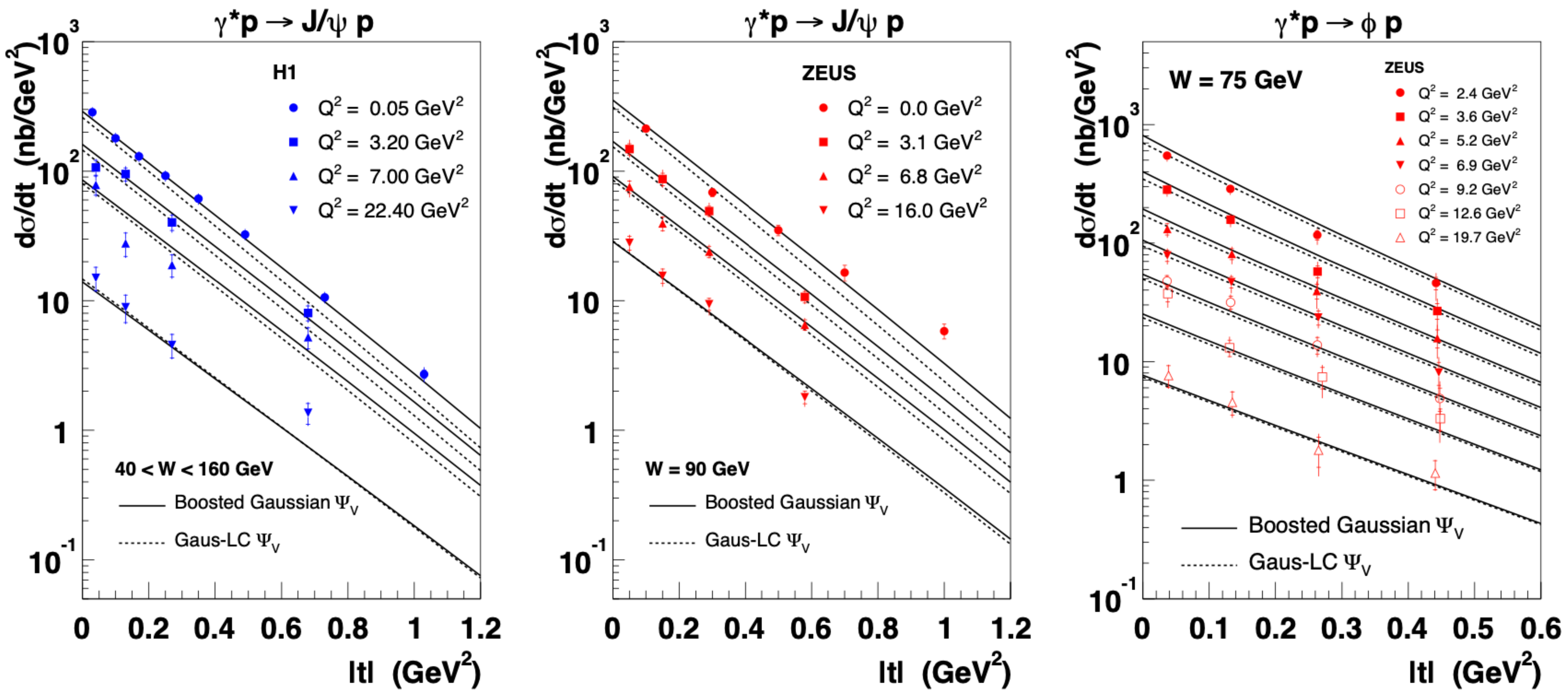

H. Kowalski, L. Motyka and G. Watt, Phys. Rev. D 74, (2006), 074016.

Virtuality dependent PDF

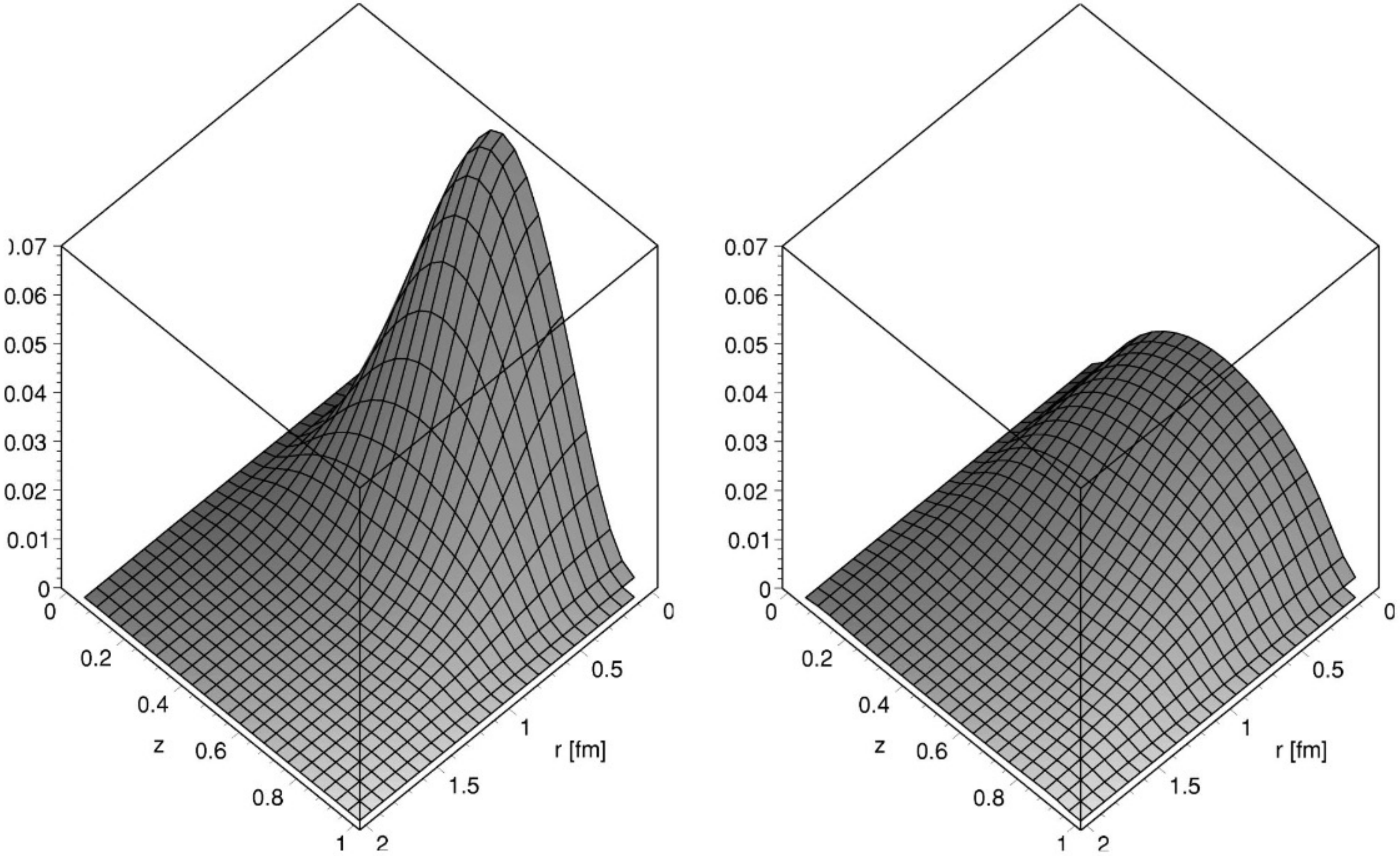

FIG. 6. The ρ wave functions $|\Psi^L|^2$ (left) and $|\Psi^T|^2$ (right) in the boosted Gaussian model with the quark mass used in the FKS dipole model.

J. R. Forshaw, R. Sandapen and G. Shaw, Phys. Rev. D 69, 094013 (2004).